1 **Current Understanding of the Driving Mechanisms for Spatiotemporal**
2 **Variations of Atmospheric Speciated Mercury: A Review**
3
4 Huiting Mao[1*], Irene Cheng[2], and Leiming Zhang[2]
5
6 [1]Department of Chemistry, State University of New York College of Environmental Science and
7 Forestry, Syracuse, NY 13210
8 [2]Air Quality Research Division, Science and Technology Branch, Environment and Climate
9 Change Canada, Toronto, M3H 5T4, Canada
10
11 [*]Corresponding author: hmao@esf.edu
12
13

Abstract

Atmospheric mercury is a global pollutant and thought to be the main source for mercury in oceanic and remote terrestrial systems, where it becomes methylated and bioavailable, and hence atmospheric mercury pollution has global consequences for both human and ecosystem health. Understanding of spatial and temporal variations of atmospheric speciated mercury can advance our knowledge of mercury cycling in various environments. This review summarized spatiotemporal variations of total gaseous mercury or gaseous elemental mercury (TGM/GEM), gaseous oxidized mercury (GOM), and particulate-bound mercury (PBM) in various environments including oceans, continents, high elevation, the free troposphere, and low to high latitudes. In the marine boundary layer (MBL), the oxidation of GEM was generally thought to drive the diurnal and seasonal variations of TGM/GEM and GOM in most oceanic regions, leading to lower GEM and higher GOM from noon to afternoon and higher GEM during winter and higher GOM during spring-summer. At continental sites, the driving mechanisms of TGM/GEM diurnal patterns included surface and local emissions, boundary layer dynamics, GEM oxidation, and for high elevation sites mountain-valley winds, while oxidation of GEM and entrainment of free tropospheric air appeared to control the diurnal patterns of GOM. No pronounced diurnal variation was found for Tekran measured PBM at MBL and continental sites. Seasonal variations in TGM/GEM at continental sites were attributed to increased winter combustion and summertime surface emissions, and monsoons in Asia, while those in GOM controlled by GEM oxidation, free tropospheric transport, anthropogenic emissions, and wet deposition. Increased PBM at continental sites during winter was primarily due to local/regional coal and wood combustion emissions. Long-term TGM measurements from the MBL and continental sites indicated an overall declining trend. Limited measurements suggested

2

38   TGM/GEM increasing from the southern to northern hemisphere due largely to the vast majority

39   of Hg emissions in the NH, and the latitudinal gradient was insignificant in summer probably as

40   a result of stronger meridional mixing. Aircraft measurements showed no significant vertical

41   variation in GEM over the field campaign regions; however depletion of GEM was observed in

42   stratospherically influenced air masses. In examining the remaining questions and issues,

43   recommendations for future research needs were provided, and among them is the most

44   imminent need for GOM speciation measurements and fundamental understanding of multiphase

45   redox kinetics.

46

47

48   **1. Introduction**

49   Atmospheric mercury (Hg) is a pervasive toxic with comparable natural and

50   anthropogenic sources (UNEP, 2013). It is operationally defined in three forms, gaseous

51   elemental mercury (GEM), gaseous oxidized mercury (GOM), and particulate-bound mercury

52   (PBM). In most environments GEM comprises >95% of total gaseous mercury (TGM =

53   GEM+GOM) with lifetime of 0.5 – 1 year (Driscoll et al., 2013). Besides emissions, GOM and

54   PBM are largely formed from oxidation of GEM, with lifetimes of hours to weeks (Cole et al.,

55   2014). They are highly soluble, and their wet and dry deposition is a major input of Hg to

56   ecosystems and oceans followed by bioaccumulation, where Hg can enter human bodies through

57   the food chain. To ultimately regulate anthropogenic emissions of Hg in order to control the

58   ambient atmospheric concentration of Hg, it is imperative to understand Hg cycling between the

59   atmosphere, ecosystems, and oceans.

60   The pathways of Hg cycling include chemical transformation and transport via air and

61   water in various systems as illustrated in Subir et al. (2011). Mercury can be chemically

62   transformed from one species to another through oxidation/reduction reactions, complex

63   formation, phase transitions, biodegradation, and surface and heterogeneous interactions with

64   aerosols, clouds, snow, and ice. Mercury can also be redistributed between geographic locations

65   and spheres through physical processes such as wind, water runoff, dry and wet deposition, and

66   volatilization. In addition, natural and anthropogenic sources of Hg are distributed vastly uneven

67   as a result of anthropogenic activities and land surface types. The eventual effect of all these

68   processes, some of which are in fact sinks, and sources is manifested in the great heterogeneity

69   of temporal and spatial variations of atmospheric Hg concentrations observed in numerous

70   studies (Sprovieri et al, 2010b, references therein; references in Tables S1 – S7 in the

71   supplementary information (SI)). Characterization and intercomparison of such variations for

72   different geographic and chemical environments can provide a gateway to our understanding of

73   Hg cycling.

74   Numerous measurement studies in the literature have shown distinctly different

75   spatiotemporal variations of GEM, GOM, and PBM in the following environments:

76   • Marine boundary layer (MBL)

77   • Land: urban, rural, and remote

78   • High elevation, high altitude

79   • Low, mid-, and high latitudes

80   owing to their respective atmospheric chemical composition, sources, and meteorological

81   conditions. Such differences were attributed to natural and anthropogenic sources of not only Hg

82   but also other reactive chemical compounds that are involved in Hg cycling, meteorological

83   conditions, and chemistry, all of which were highly dependent on geographic locations and

84   surrounding land surface types. Therefore, it is highly complex to delineate the effects of

85   controlling factors determining observed spatiotemporal variations of Hg concentrations.

86   Sprovieri et al. (2010b) reviewed the state of global mercury measurements focusing on

87   instrumentation and techniques, and ranges of concentration levels in studies from different

88   continents and oceanic regions up to 2009. Atmospheric Hg research has since continued to

89   flourish, and in particular longer datasets accumulated in several regions have become available

90   for temporal variability characterization so as to understand the driving mechanisms for such

91   variabilities. Also of importance is the efficacy of emission reductions that have been

92   implemented in North America and Europe for nearly two decades and over shorter periods in

93   East Asia. This paper is, different from Sprovieri et al. (2010b), aimed to provide a global

94   picture of spatiotemporal variations of speciated Hg using measurement-based studies in the

95   literature over ocean, over land, by altitude, and by latitude, and further glean insight on

96   important factors that could potentially contribute to the observed variations.

97   It should be noted that ***___units were converted for a standard atmosphere___*** for comparison.

98   One more cautionary note is that Hg data in earlier studies had coarser temporal resolution than

99   in more recent studies, and hence the comparisons should be viewed with this caveat in mind.

100   Though the earlier studies tended to have orders of magnitude larger concentrations, suggesting

101   at higher temporal resolution those concentrations would have been even larger.

102   **2. Marine Boundary Layer**

103   Measured TGM/GEM, GOM, and PBM concentrations in the MBL globally were

104   summarized in Tables S1 – S3 of the supplementary information (SI). Spatiotemporal variations

105   in speciated Hg and the potential causes for these variations were summarized with respect to

106   their ambient concentration levels, continental (including anthropogenic) influence, hemispheric

5

107   gradient, diurnal to annual cycles, and long term trends, accompanied by discussions on potential

108   causal mechanisms.

109   ***2.1 TGM/GEM***

110   TGM and GEM in the MBL atmosphere have been measured since the late 1960s. Near

111   the surface in most environments, except polar springtime and Dead Sea mercury depletion

112   events (MDEs) when strong GEM oxidation occurs, the difference between TGM and GEM was

113   small to negligible (e.g., Temme et al., 2003a; Mao and Talbot, 2012). Concentrations were

114   generally higher in near-coastal regions due largely to anthropogenic influence, which under

115   certain meteorological conditions could extend to even open oceans. Natural emissions

116   including biomass burning, volcanic, and oceanic emissions were suggested to be of influence in

117   some studies. It was also found that meteorological conditions could play important roles in

118   determining ambient concentrations of TGM/GEM via transport, PBL dynamics, and solar

119   radiation, especially in regions nearing emission sources such as the Mediterranean and in

120   springtime Polar Regions.   Long term trends have varied over different time periods, speculated

121   to be associated with changing anthropogenic emissions, legacy emissions, and photooxidation.

122   2.1.1 Concentration Metrics

123   The mean concentrations of TGM/GEM observed over varying time periods reported

124   from the studies in the literature ranged from 1.05 ng m^{-3} over the *Antarctic* Ocean to 2.34 ng m^{-3}

125   over the *West Pacific seas*, as shown in Table S1 (references therein). The concentration

126   averaged for each oceanic region calculated using the values reported from all the studies was

127   the lowest at 1.53 ng m^{-3} over the *Antarctic* Ocean and the largest at 2.36 ng m^{-3} over the *West*

128   *Pacific seas* (**Fig. 1a**). The range of 0.05 – 29 ng m^{-3} over the Atlantic (**Fig. 1a**), obtained from

129   individual studies, appeared to be the largest, although the maximum concentration was from a

130   single event influenced by forest fires in Quebec, Canada at a long term site in the MBL 20 km

131   from the coast of southern New Hampshire, USA (Mao and Talbot, 2012). With that single

132   event removed, the TGM/GEM concentrations were much more variable in the MBL of the

133   *Mediterranean Sea* and its nearby seas (Table S1; references therein).

134   Atmospheric Hg over the *Atlantic* Ocean has been studied most extensively compared to

135   other oceans, largely via shipboard measurements. Concentrations of TGM/GEM ranged from

136   0.05 ng m^{-3} (15-minute average) in Cape Point, South Africa (Brunke et al., 2010) to 29 ng m^{-3}

137   (5-minute average) near the shore of southern New Hampshire, USA (Mao and Talbot, 2012). In

138   the earliest shipboard global study of atmospheric Hg, Seiler et al. (1980) found highly variable

139   TGM concentrations (1 – 10 ng m^{-3}, 2-4 h average) averaged at 2.8 ng m^{-3} between Hamburg

140   (54°N, 10°E) and Santo Domingo (20°N, 67°W) across the Atlantic Ocean over 11 October - 1

141   November 1973. It should be noted that early studies used very different measurement

142   techniques and hence the magnitude needs to be considered with discretion. During the following

143   40 years, most studies reported TGM/GEM ranging from below LOD to a few ng m^{-3} and higher

144   concentrations in near-coastal regions (Table S1; references therein). The *first* measurements of

145   Hg species was a one month shipboard study over the *South Atlantic* Ocean during polar summer

146   (February) 2001 by Temme et al. (2003b). Their measurements (5-min – 15-min average data)

147   during the cruise from Neumayer to Punta Arenas exhibited very small variation with TGM

148   averaged at 1.1±0.2 ng m^{-3} and no significant difference between TGM and GEM. Relatively

149   homogeneous distributions of TGM/GEM were observed over open waters in the *South Atlantic*

150   with mean values hovering around 1 ng m^{-3} and standard deviation <0.3 ng m^{-3} compared to

151   larger mean values (1.3 – ~3 ng m^{-3}) over the *North Atlantic*.

152   Over the *Pacific* Ocean, 1-min to 15-min TGM/GEM concentrations measured over the

153 North and South *Pacific* Ocean ranged from 0.3 ng m^{-3} over 40° – 45°N in July – September

154 2008 (Kang and Xie, 2011) to 7.21 ng m^{-3} in the Los Angeles Port on 27 May 2010 (Weiss-

155 Penzias et al., 2013), with generally higher concentrations near coasts and lower ones over open

156 oceans (Table S1; reference therein). The distribution of TGM/GEM over the South *Pacific*

157 appeared to be quite heterogeneous, where Xia et al. (2010) measured TGM averaged at

158 2.20±0.67 ng m^{-3}, a factor of 2 higher than those in Soerensen et al. (2010) that measured a mean

159 of 1.03 ±0.16 ng m^{-3}.

160 Over the *South China Sea, the Yellow Sea,* and other neighboring seas, located on the

161 Eastern Asian continental margin in the tropical-subtropical western North Pacific, elevated

162 concentrations of TGM/GEM were observed with mean values varying over 2.08 – 2.62 ng m^{-3}

163 (Fu et al., 2010; Nguyen et al., 2011; Ci et al., 2011) (Table S1). TGM concentrations over the

164 *Mediterranean Sea, Adriatic Sea, Dead Sea, Augusta Basin,* and *Baltic Sea* ranged from 0.4 to

165 11 ng m^{-3} (Table S1; references therein).

166 A few studies on Hg over the *Indian* Ocean (Soerensen et al., 2010; Xia et al., 2010; Witt

167 et al.; 2010; Angot et al., 2014) reported a concentration gradient of TGM with increasing

168 concentrations at more northern locations closer to the inter-tropical convergence zone (ITCZ),

169 with a mean concentration of 1.24±0.06 ng m^{-3} over 9°S - 21°S latitudes (Witt et al., 2010).

170 Studies on TGM/GEM over the *Arctic* Ocean showed fairly constant concentrations in

171 January and August – December and reported MDEs in spring and summertime annual

172 maximums (Lindberg et al., 2002; Aspmo et al., 2006; Sommar et al., 2010; Steffen et al., 2013;

173 Yu et al., 2014). During the 1998 – 2001 Barrow Atmospheric Mercury Study (BAMS), daily

174 average GEM concentrations ranged from <0.2 to ~3.7 ng m^{-3}, averaged between 1.5 – 2 ng m^{-3}

175 in January and mid-August – December (Lindberg et al., 2002). The means and ranges measured

176   in summer 2004, 2005, and 2012 (Aspmo et al., 2006; Sommar et al., 2010; Yu et al., 2014) were

177   well within the 1999 summertime range of Lindberg et al. (2002) (Table S1). Different

178   concentrations of GEM over sea ice–covered (1.81±0.43 ng m^{-3}) vs. sea ice-free (1.55±0.21 ng

179   m^{-3}) Arctic Oceanic waters were measured by Sommar et al. (2010) in summer 2005. In spring

180   2009 (14 – 26 March) a mean 5-min GEM concentration of 0.59 ng m^{-3} was measured with a

181   range of 0.01–1.51 ng m^{-3} over sea ice on the Beaufort Sea near Barrow, Alaska, which appeared

182   to be depleted compared to annual Arctic ambient boundary layer concentrations (Steffen et al.,

183   2013).

184   In the *Antarctica*, the first study, conducted by de More et al. (1993), reported a mean

185   TGM concentration of 0.55±0.28 ng m^{-3} and a range of 0.02 - 1.85 ng m^{-3} (24-48 h) at Ross

186   Island during 1987 – 1989. Over November 2000 – January 2001, Sprovieri et al. (2002)

187   reported a similar range but a mean of 0.9±0.3 ng m^{-3}, twice larger than that of de More (1993) a

188   decade earlier. Similar means and ranges of TGM/GEM concentrations were measured by

189   Ebinghaus et al. (2002b), Temme et al. (2003b), Soerensen et al. (2010), and Xia at al. (2010).

190   Similar mean values but a much wider range (0.02 – 3.07 ng m^{-3}) were found in the multi-year

191   dataset in Pfaffhuber et al. (2012) (Table S1).

192   2.1.2 Hemispheric Difference

193   Hemispheric gradient over the *Atlantic* and *Pacific* Ocean has been reported since the

194   1980s, with higher concentrations in the North Atlantic attributed to anthropogenic and biomass

195   burning emissions (Seiler et al, 1980; Slemr et al., 1981, 1985, 1995; Slemr and Langer, 1992;

196   Fitzgerald et al., 1996; Lamborg et al., 1999; Temme et al., 2003a; Chand et al., 2008; Xia et al.,

197   2010; Soerensen et al., 2010; Müller et al., 2012). An average gradient of 0.37 ng m^{-3} in TGM

198   was measured in October – November 1973 (Seiler et al., 1980). Measurements from the same

199   cruise paths from Hamburg (54°N) to Buenos Aires (35°S) in 1977, 1978 – 1980, 1992, and

200   1994 consistently showed TGM hemispheric difference, 1.56±0.32 and 1.05±0.22 ng m^{-3} in the

201   NH and SH, respectively, in 1977, increased to 2.25±0.41 and 1.50±0.30 ng m^{-3} in 1992

202   followed by significant decreases to 1.79±0.41 and 1.18±0.17 ng m^{-3} in 1994 (Slemr et al., 1981,

203   1985, 1995; Slemr and Langer, 1992). The hemispheric difference from a NH average of

204   1.32±0.16 ng m^{-3} in summer 2006 and 2.61±0.36 ng m^{-3} in spring 2007, and a SH average of

205   1.27±0.2 ng m^{-3} measured by Soerensen et al. (2010) was close to the 1978 – 1980 hemispheric

206   gradient in Slemr et al. (1985) but lower than the 1990 value in Slemr and Langer (1992).

207   Over the *Pacific* a hemispheric gradient of ~0.4 ng m^{-3} was found in early studies by

208   Seiler et al. (1980) and Fitzgerald et al. (1984). Higher concentrations but similar magnitude of

209   hemispheric difference of TGM was measured in December 2007 by Xia et al. (2010) with a

210   mean of 1.746±0.513 ng m^{-3} over the *North Pacific* and 1.471±0.842 ng m^{-3} over the *South*

211   *Indian* Ocean (Note: their cruise passed through the South Indian instead the South Pacific).

212   Around the same time, Soerensen et al. (2010) measured nearly twice lower concentrations over

213   the *South Pacific* (1.11±0.11 ng m^{-3} along the Chilean Coast and up to 1.33±0.24 ng m^{-3} near

214   East Australia) than the *North Atlantic* concentrations (mean values of 2.26 and 2.86 ng m^{-3} over

215   23°N – 59°N; no measurements over the *North Pacific* in the study) from the same study.

216   Studies found higher TGM concentrations up to ~2.3 ng m^{-3} over *the equatorial Pacific*

217   in October 1980, markedly higher (>0.5 ng m^{-3}) than those outside this region (Fitzgerald et al.,

218   1984; Kim and Fitzgerald, 1988). However, Wang et al. (2014) found no sustained high GEM

219   concentrations indicative of persistently enhanced biotic mercury evasion from the upwelling

220   region over the Galápagos Islands in the equatorial Pacific during February – October 2011.

221   They found GEM concentrations averaged at 1.08±0.17 ng m^{-3}, twice lower than the earlier ones.

222   2.1.3 Temporal Variations from Diurnal Cycle to Long-term Trend

223   2.1.3.1 Diurnal variation

224   Early studies on TGM over the *Atlantic* Ocean showed one order of magnitude larger

225 diurnal amplitude than that in more recent studies, with daily peaks of 5 ng m^{-3} at noon and

226 amplitude of 2-3 ng m^{-3} across the North and South Atlantic in Seiler et al. (1980). Yet none was

227 observed by Slemr et al. (1981, 1985) and Slemr and Langer (1992). Measurements of TGM at

228 Cape Point, South Africa (Brunke et al., 2010) and GEM at Appledore Island, Maine, USA (Mao

229 and Talbot, 2012) exhibited pronounced diurnal variation in summer with daily peaks

230 (minimums) before sunrise (in the late afternoon) and amplitudes of 0.8 ng m^{-3} and ~10 ppqv

231 (~0.09 ng m^{-3}) for the two sites, respectively.

232   The opposite diurnal pattern with significant amplitude was observed over the *Pacific*

233 (Fitzgerald et al., 1984; Weiss-Penzias et al., 2003, 2013; Kang and Xie, 2011; Tseng et al., 2012;

234 Wang et al., 2014) with daily peaks ranging from 0.7 ng m^{-3} (5-min) over the Japan Sea (Kang

235 and Xie, 2011) to 2.25 ng m^{-3} (unknown time resolution) in the equatorial region (Fitzgerald et

236 al., 1984). The most pronounced diurnal variation in TGM was reported in Fitzgerald et al. (1984)

237 with daily amplitude of 0.7 ng m^{-3} in the equatorial region (4°N – 10°S). Similar pattern and

238 magnitude of GEM diurnal variation was observed by Tseng et al. (2012) over the *South China*

239 *Sea* during May 2003 – December 2005, especially in warm seasons. Opposite patterns were

240 observed in Weiss-Penzias et al. (2003, 2013). Laurier et al. (2003) found no diurnal variation

241 during a cruise from Osaka, Japan to Honolulu, Hawaii over 1 May 2002 – 4 June 2002.

242   Over the *Arctic* diurnal variation of GEM was observed by Lindberg et al. (2002) with

243 noontime minimums in spring and summer, diurnal amplitude ~2 ng m^{-3} on a typical day in

244 January – June. On the other hand, the shipboard measurements from Sommar et al. (2010)

245   suggested very small near none diurnal variation. Similarly, no diurnal variation was found over

246   the *Antarctica* (Pfaffhuber et al., 2012), except one case with influence of in situ human activity.

247   2.1.3.2 Seasonal to Annual Variation

248   Annual cycles of TGM/GEM were reported over *the Atlantic* in both hemispheres.

249   Annual cycles with an annual maximum in austral summer and a minimum in austral winter and

250   average amplitude of 0.134 ng m^{-3} were observed at Cape Point, South Africa (Slemr et al., 2008;

251   Brunke et al., 2010). Opposite annual variation with higher (lower) concentrations in winter

252   (summer) was measured over the *North Atlantic*, such as Mace Head (amplitude 0.097 ng m^{-3}), a

253   remote site on the west coast of Ireland adjacent to the North Atlantic (Ebinghaus et al., 2002a)

254   and the Appledore Island (25 ppqv, i.e. ~0.2 ng m^{-3}) site in Mao and Talbot (2012). Similarly,

255   significant seasonal variation in NH with an annual minimum in July and maximum in January –

256   March and amplitude of 0.3 – 0.4 ng m^{-3} was measured in a global cruise (Soerensen et al., 2010).

257   Average seasonal difference of 0.19 ng m^{-3} GEM concentrations over the *Pacific* were

258   observed by Wang et al. (2014) with the highest and most variable concentrations over February

259   – May 2011 and the lowest and least variable in October over the Galápagos Islands during 12

260   November 2011 – 11 December 2011. In contrast, a *lack* of seasonal variation in GEM was

261   reported by Weiss-Penzias et al. (2003) using a subset of data of marine origin extracted from

262   one year speciated Hg data (May 2001 – May 2002) at the Cheeka Peak Observatory on the east

263   coast of the Pacific. This was uncharacteristic of midlatitudinal NH sites, but significant

264   interannual variation was noted in this study.

265   Distinct annual variation in GEM over the *South China Sea* was observed in the cruise

266   study by Tseng et al. (2012) over May 2003 – December 2005. The winter maximum was

267   5.7±0.2 ng m^{-3} and summer minimum 2.8±0.2 ng m^{-3}, 2-3 times higher than global background

268   levels. Difference of 0.4 ng m^{-3} in seasonal average GEM was quantified with higher

269   concentrations in the summer than in the autumn over the *Adriatic Sea* (Sprovieri et al., 2010)

270   and a factor of two less over the *Augusta Basin* (Bagnato et al., 2013). The study by Obrist et al.

271   (2011) was the first to show the occurrence of mercury depletion events (MDEs) in midlatitudes

272   with GEM down to 22 ppqv (0.2 ng m^{-3}) most frequently in summer in the boundary layer of the

273   *Dead Sea*, as opposed to MDEs, as commonly known, occurring in the springtime *Arctic* and

274   *Antarctic* only.

275   Annual variation of GEM over the *Indian* Ocean was reported in Angot et al. (2014) with

276   higher concentrations in winter (1.06±0.09 ng m^{-3}) and lower in summer (1.04±0.07 ng m^{-3}),

277   opposite of those at Cape Point (Slemr et al., 2008) and Galapagos Islands (Wang et al., 2014)

278   with annual amplitude an order of magnitude smaller.

279   Annual maximum concentrations of GEM occurred in summer over the *Arctic* Ocean and

280   frequent MDEs with GEM depleted to near zero in spring (Lindberg et al., 2002; Aspmo et al.,

281   2006; Cole et al., 2013; Moore et al., 2013). Lindberg et al. (2002) observed GEM

282   concentrations up to 4 ng m^{-3} in June 2000 compared to 1.82±0.24 ng m^{-3} in summer 2004

283   (Aspmo et al., 2006) and 1.23±0.61 ng m^{-3} in summer 2012 (Yu et al., 2014).

284   Seasonal variation in *Antarctic* Hg suggested large variation in TGM/GEM in spring due

285   to the occurrence of MDEs. The longest continuous data record in the Antarctic started in

286   February 2007 at the Norwegian Antarctic Troll Research Station (TRS) in Queen Maud Land

287   near the Antarctic coast (Pfaffhuber et al., 2012). Concentrations were fairly constant hovering

288   at ~1±0.07 ng m^{-3} in late fall through winter and highly variable ranging from 0.02 to 3.04 ng m^{-3}

289   with a mean of 0.86±0.24 ng m^{-3} in spring and summer (Pfaffhuber et al., 2012), close to the

290   values from 6 years earlier in Sprovieri et al. (2002) and Temme et al. (2003b).

291   2.1.3.3 Long-term Trends

292   Long-term trends in TGM over the *Atlantic* varied during different time periods of the

293 past decades. TGM concentrations averaged over latitudes from Hamburg, Germany to Punta

294 Arenas, Chile were increasing at a rate of $1.46\pm0.17\%$ yr^{-1} from 1970 to 1990 (Slemr and Langer,

295 1992) followed by a 22% decrease from 1990 to 1994 (Slemr et al., 1995). In similar latitudinal

296 coverage but over a wider longitudinal span during three cruises in September – November 1996,

297 December 1999 – March 2000, and February 2001, TGM concentrations were averaged at

298 1.26 ± 0.1 ng m^{-3} (Temme et al., 2003a), comparable to the 1977 – 1980 (Slemr et al., 1985) and

299 1994 concentrations (Slemr et al., 1995) but lower than the 1990 ones (Slemr et al., 1992). Over

300 September 1995 – December 2001, a slight increase (4%) in TGM was observed at Mace Head

301 (Ebinghaus et al., 2002a). In the *South Atlantic* at Cape Point a small but significant decrease

302 was reported in TGM annual median from 1.29 ng m^{-3} in 1996 to 1.19 ng m^{-3} in 2004 (Slemr et

303 al., 2008), and at an about three times faster decreasing rate (-0.034 ± 0.005 ng m^{-3} yr^{-1}) over 1996

304 – 2008 (Slemr et al., 2011). A statistically significant decreasing trend of -0.028 ± 0.01 ng m^{-3} yr^{-1}

305 ^{1} ($\sim$1.6-2.0% yr^{-1}) in TGM over the North *Atlantic* was reported for the same time period at Mace

306 Head, Ireland (Ebinghaus et al., 2011). In an updated study, Weigelt et al. (2015) presented a

307 relatively smaller decreasing trend of -0.016 ± 0.002 ng m^{-3} yr^{-1} in monthly median marine GEM

308 concentrations over 1996 – 2013. In Soerensen et al. (2012) a steep 1990–2009 decline of -

309 0.046 ± 0.010 ng m^{-3} yr^{-1} (-2.5% yr^{-1}) was found in TGM over the *North Atlantic* (steeper than at

310 NH land sites) but no significant decline over the *South Atlantic*. A recent comparison by Slemr

311 et al. (2015) found smaller trends during shorter time periods and a possible increasing trend at

312 Cape Point for the period 2007–2013, qualitatively consistent with the trend changes observed at

313 Mace Head (Weigelt et al., 2015).

314   Over the *Arctic* Ocean, weak or insignificant declines in TGM at rates of -0.007±0.019

315   and -0.003±0.012 ng m^{-3} yr^{-1} were found at Alert and Zeppelin, respectively, during 2000 – 2009,

316   significantly smaller than the trends at midlatitude sites (Ebinghaus et al., 2011; Slemr et al.,

317   2011; Soerensen et al., 2012; Cole et al., 2013; Berg et al., 2013; Weigelt et al., 2015).

318   TGM/GEM concentrations over the *Antarctic* Ocean appeared to have increased from the 1980s

319   to the 2000s (Ebinghaus et al., 2002b; Temme et al., 2003b; Soerensen et al., 2010; Xia et al.,

320   2010; Pfaffhuber et al., 2012), and no significant trend was detected over 2007 – 2013 (Slemr et

321   al., 2015).

322   2.1.4 Mechanisms Driving the Observed Temporal Variabilities

323   2.1.4.1 Causes for Episodic Higher Concentrations

324   It has been hypothesized that anthropogenic, biomass burning, and volcanic emissions

325   caused higher concentrations over open waters and near-coastal regions in many cases. Such

326   influences on the atmospheric concentration of Hg was demonstrated using backward trajectories

327   and correlations of TGM/GEM with carbon monoxide (CO), ^{222}Rn, black carbon, sulfur dioxide

328   (SO$_2$), and dimethylsulfide (DMS) (Williston, 1968; Seiler et al., 1980; Fitzgerald et al., 1981;

329   Fitzgerald et al., 1984; Kim and Fitzgerald, 1988; Slemr et al., 1981; Slemr et al., 1985; Slemr

330   and Langer, 1992; Slemr, 1996; Lamborg et al., 1998; Sheu and Mason, 2001; Laurier and

331   Mason, 2007; Soerensen et al., 2010; Mao and Talbot, 2012; Müller et al., 2012; Xia et al., 2010;

332   Chand et al., 2008; Kang and Xie, 2011; Weiss-Penzias et al., 2013; Fu et al., 2010; Nguyen et

333   al., 2011; Ci et al., 2011; Bagnato et al., 2013; Kotnik et al., 2014). Some studies also suggested

334   that oceanic evasion was an important source contributing to higher concentrations (Seiler et al.,

335   1980; Pirrone et al., 2003; Sigler et al., 2009b), while others thought otherwise (Slemr et al.,

336   1981, 1985; Slemr and Langer, 1992). Strong photoreduction could have caused higher

15

337   TGM/GEM concentrations under sunny, warm and dry conditions with lower amounts of

338   precipitation in the Mediterranean Sea region (Pirrone et al., 2003; Sprovieri et al., 2003;

339   Sprovieri and Pirrone, 2008). These influences often occurred in multitude simultaneously

340   leading to elevated ambient Hg concentrations.

341   2.1.4.2 Diurnal Variation

342   Nearly in all studies diurnal variation over the *Atlantic, Pacific*, and *Arctic* was found to

343   be most pronounced in warm seasons, i.e. spring and/or summer. Different combinations of

344   oceanic emissions, photooxidation, biological production, and meteorology were suggested to

345   work together shaping the observed patterns in different oceanic regions. The pattern with

346   daytime peaks was attributed to oceanic emissions and biological production in sea water (Seiler

347   et al., 1980; Fitzgerald et al., 1984; Tseng et al.; 2012; Wang et al., 2014), which was supported

348   by the concurrent measurements of dissolved elemental Hg (Tseng et al., 2012). The opposite

349   pattern with daytime minimums was associated with photooxidation of GEM by abundant

350   halogen radicals and meteorological conditions (Lindberg et al., 2002; Brunke et al., 2010; Mao

351   and Talbot, 2012; Weiss-Penzias et al., 2003, 2013). The most pronounced diurnal variation in

352   TGM in the equatorial area (4°N – 10°S) was demonstrated to be caused by biological

353   production (Fitzgerald et al., 1984).

354   However, Mao et al. (2012) suggested that the predominant effect of oceanic evasion on

355   ambient GEM concentrations was episodic, not necessarily diurnal, because they found, among

356   all physical parameters, the only significant correlation GEM had was with wind speed

357   exceeding15 m s^{-1} at a marine location, which occurred rather sparsely. This was corroborated

358   by Sigler et al. (2009b) suggesting enhanced oceanic evasion at a rate of ~7 ppqv hr^{-1} (0.063 ng

359   m^{-3}) leading to 30 – 50 ppqv (0.27-0.45 ng m^{-3}) increases in coastal and inland GEM

360 concentrations in southern New Hampshire, USA during the April 2007 Nor'easter.

361   In the study by Laurier et al. (2003) the lack of diurnal variation over the *Pacific* was

362 speculated to be caused by continuous evasion from surface water. Over the *Arctic*, unlike the

363 distinctive diurnal pattern with noontime peaks in the study by Lindberg et al. (2002), very small

364 near none diurnal variation in GEM was manifested in the shipboard measurements of Sommar

365 et al. (2010) and was speculated to result from low in situ oxidation of GEM. No diurnal

366 variation was found over the *Antarctica* due possibly to lack of diurnally varying sources and

367 sinks (Pfaffhuber et al., 2012), except one case with in situ human activity.

368   2.1.4.3 Seasonal to Annual Variation

369   Annual cycles of TGM/GEM in the MBL differed between various oceanic regions and

370 were suggested to be driven predominantly by oceanic evasion, biomass burning, anthropogenic

371 emissions, interhemispheric flux, and/or meteorological conditions (Slemr et al., 2008;

372 Ebinghaus et al., 2002a,b; Sigler et al., 2009a; Brunke et al., 2010; Soerensen et al., 2010; Mao

373 and Talbot, 2012; Angot et al., 2014; Wang et al., 2014). Annual cycles of TGM/GEM with an

374 annual maximum in summer and a minimum in winter observed at Cape Point, South Africa in

375 the *South Atlantic* MBL was hypothesized to be driven predominantly by oceanic emissions,

376 biomass burning, and anthropogenic activities (Brunke et al., 2010), and interhemispheric flux

377 (Slemr et al., 2008; Brunke et al., 2010). Higher concentrations of GEM in the summer over the

378 *Adriatic Sea* (Sprovieri et al., 2010) and over the *Augusta Basin* (Bagnato et al., 2013) were

379 suggested to be caused by stagnant meteorological conditions in the former study and enhanced

380 evasion from sea water in the latter. *Opposite annual variation* with higher (lower)

381 concentrations in winter (summer) was proposed to be determined largely by meteorology

382 (Ebinghaus et al., 2002a, 2011) and photochemical oxidation of GEM (Mao and Talbot, 2012).

383   The same annual cycle over the *Indian* Ocean was speculated to be a result of long range

384   transport of air masses originated from southern Africa biomass burning during the winter

385   months (July – September), and low GEM associated with southerly polar and marine air masses

386   from the remote southern Indian Ocean (Angot et al., 2014). Frequent MDEs in the summertime

387   Dead Sea MBL were observed to be often concurrent with varying concentrations of bromine

388   oxide (BrO) and high temperatures up to 45°C (Obrist et al., 2011). Such high temperatures

389   seemed to be contradictory to the general understanding that Br-initiated GEM oxidation tends to

390   go forward under very cold conditions at temperature < -40°C. Despite that, the authors

391   suggested that Br species were the major oxidants of GEM during depletion events, even when

392   constantly high temperatures were accompanied by sometimes low BrO concentrations.

393   Springtime large variation in *Arctic* and *Antarctic* TGM/GEM was caused by the

394   occurrence of MDEs. Polar MDEs have been generally linked to reactive Br-initiated GEM

395   oxidation in spring when Br explosion occurs producing abundant reactive Br (Schroeder et al.,

396   1998; Ebinghaus et al., 2002b; Lindberg et al., 2002; Temme et al., 2003b; Mao et al., 2010;

397   Steffen et al., 2013; Moore et al., 2014). For Antarctic MDEs, Ebinghaus et al. (2002b) found a

398   strong positive correlation between TGM and O_3 over August – October, accompanied by

399   enhanced Global Ozone Monitoring Experiment (GOME) column BrO. Compared to Arctic

400   MDEs, the first Antarctic MDE occurred about 1-2 months earlier, probably due to the lower

401   latitude of the monitoring site and sea ice, the former allowing earlier sunrise and the latter

402   conducive to Br/BrO formation. Temme et al. (2003b) found that the air masses reaching the

403   station during MDEs had a maximum contact with sea ice (coverage >40%) over the South

404   Atlantic Ocean, which was speculated to contain abundant reactive Br released from sea salt

405   associated with sea ice or sea salt aerosols.

406   Summertime annual maximums of GEM over the *Arctic* and *Antarctic* Ocean were

407   generally associated with enhanced evasion of GEM and from GOM reduction in snow resulting

408   from maximum exposed sea water after snow/ice melt (Lindberg et al., 2002; Aspmo et al., 2006;

409   Soerensen et al., 2010; Cole et al., 2013; Moore et al., 2014), which was also suggested using

410   model simulations by Dastoor and Durnford (2014). A different mechanism of riverine

411   contribution was hypothesized in Fischer et al. (2012) using an atmosphere-ocean coupled model.

412   Yu et al. (2014) observed high TGM concentrations concurrent with low salinity, CO, and high

413   chromophoric dissolved organic matter (CDOM) over the ice-covered central Arctic Ocean and

414   speculated that the relatively high CDOM concentrations associated with river runoff could

415   enhance Hg^{2+} reduction. Moreover they related the summer monthly variability in TGM

416   concentrations to less chemical loss.

417   2.1.4.4 Long-term Trends

418   Four *hypotheses* were made to explain the observed decreasing trends in TGM/GEM

419   during the past decades. First, the global decreasing trend was caused by decreased reemission

420   of legacy mercury as a result of a substantial shift in the biogeochemical cycle of Hg through the

421   atmospheric, oceans, and soil reservoirs, although exactly what may have caused this shift

422   remained unexamined (Slemr et al., 2011). Second, the decreasing trend was linked to

423   increasing tropospheric O_3 (Ebinghaus et al., 2011). However, this speculation was negated by

424   the plausibility of GEM oxidation by O_3 in the atmosphere. Third, based on atmosphere-ocean

425   coupled model simulations, the decreasing trend in TGM over the North Atlantic was caused by

426   decreasing North Atlantic oceanic evasion driven by declining subsurface water Hg

427   concentrations resulting from reduced Hg inputs from rivers and wastewater and from changes in

428   the oxidant chemistry of the atmospheric MBL (Soerensen et al., 2012. However, Amos et al.

19

429   (2014) suggested that the decrease in riverine input was too small to affect Hg concentrations in

430   the open ocean let alone the declining trend in North Atlantic sea water Hg concentrations. Last,

431   a 20% decrease in total Hg emissions and 30% in anthropogenic Hg° emissions were estimated

432   for the period of 1990 – 2010, leading to the observed decreasing trends in TGM/GEM, as

433   suggested by a most recent modeling study (Zhang et al., 2016).

434   ***2.2 GOM and PBM***

435   2.2.1 Concentration Metrics

436   The mean concentrations of GOM from individual studies varied from below LOD in

437   several studies to 4018 pg m^{-3} (1-h) in the *Dead Sea* MBL (Obrist et al., 2011; Moore et al., 2013)

438   (Table S2; references therein). The GOM concentration averaged for each oceanic region based

439   on values from the literature varied from 3 pg m^{-3} over the *Atlantic Ocean* to 40 pg m^{-3} over the

440   *Antarctica*, and the largest range 0.1 – 4018 pg m^{-3} was over the *Mediterranean* Sea and its

441   neighboring seas (**Fig. 1b**). Note that the small ranges in other oceanic MBL did not necessarily

442   indicate less variability in GOM but merely a result of limited measurement data available (Table

443   S2; references therein).

444   The mean concentrations of PBM from individual studies varied from below LOD in

445   several regions to 394 pg m^{-3} (1-h) over the *Beaufort* Sea (Steffen et al., 2013) (Table S3;

446   references therein). The PBM concentration averaged for each oceanic region based on values in

447   the literature varied from 0.6 pg m^{-3} over the *Indian* to 394 pg m^{-3} over the *Arctic* Ocean (**Fig.**

448   **1c**). No ranges were provided for the *Arctic, Antarctic,* and *Indian Ocean* MBL due to limited

449   numbers of studies there. The few studies available indicated that PBM concentrations were in

450   most cases smaller and less variable than GOM.

451   The earliest shipboard measurements of GOM showed dimethyl mercury (DMM)

452   concentrations orders of magnitude larger (Slemr et al., 1981, 1985) than the total GOM

453   concentration measured in the recent two to three decades. Due to the use of very different

454   techniques in early studies, those concentrations were listed in Table S2 (references therein) but

455   were not used for comparison with more recent studies (Table S2; references therein).

456   Same as GEM, GOM concentrations tended to be higher over the North than the South

457   *Atlantic* and in near-coastal regions than open waters (Temme et al., 2003b; Mason et al., 2001;

458   Sheu and Mason, 2001; Mason and Sheu, 2002; Aspmo et al., 2006; Laurier and Mason, 2007;

459   Sigler et al. 2009b; Mao and Talbot, 2012). Hourly GOM concentrations of $1 - 30$ pg m^{-3} over

460   the *South Atlantic* Ocean from Neumayer to Punta Arenas in February 2001 (Temme et al.,

461   2003b) were $1 - 2$ orders of magnitude smaller than the concentrations (1.38 ± 1.30 pmol m^{-3}, i.e.

462   ~300 ± 280 pg m^{-3}) near Bermuda in September and December 1999 and March 2000 (Mason et

463   al., 2001). However, at around the same time average values almost an order of magnitude

464   smaller were reported at Bermuda (50 ± 43 pg m^{-3}, a few pg m^{-3} to 128 pg m^{-3}) (Mason and Sheu,

465   2002) and at a US mid-Atlantic coastal site (40 pg m^{-3}) (Sheu and Mason, 2001). In comparison,

466   GOM concentrations were an order of magnitude smaller over the open water and at higher

467   latitude (Aspmo et al., 2006; Laurier and Mason, 2007), comparable to those over the *South*

468   *Atlantic*. Similar magnitude of GOM concentrations were measured at a *North Atlantic* near

469   coastal MBL site with an average of 0.4 ppqv (~3.6 pg m^{-3}) ($0 - 22$ ppqv, i.e. $0 - 196$ pg m^{-3}, 2-h)

470   during $2007 - 2010$ (Sigler et al., 2009b; Mao and Talbot, 2012).

471   PBM concentrations (Table S3; references therein) were measured with an average of

472   1.9 ± 0.2 pg m^{-3} during the May-June 1996 *South* and *equatorial Atlantic* cruise (Lamborg et al.,

473   1999) and 1.3 ± 1.7 pg m^{-3} (<0.5 pg m^{-3} (LOD) to 5.2 pg m^{-3}) in Bermuda, 30-40 times smaller

474   than the concurrent weekly averaged GOM concentrations (Mason and Sheu, 2002; Sheu, 2001).

475   At higher *North Atlantic* latitudes, PBM concentrations were averaged at 2.4 pg m^{-3}, very close

476   to the concurrent average GOM concentrations but with a factor of 4 smaller varying from

477   <LOD to 6.3 pg m^{-3} in summer 2004 (Aspmo et al., 2006). Mao and Talbot (2012) reported

478   PBM concentrations varying from 0.09 ppqv (0.8 pg m^{-3}) in winter 2010 to 0.52 ppqv (4.6 pg m^{-3})

479   in summer 2010.

480   During the 2000s decade, concentrations of GOM over the *Pacific* decreased by around a

481   factor of 2 from 9.5 pg m^{-3} over open waters in 2002 (Laurier et al., 2003) to around 4 pg m^{-3} at a

482   remote Japanese site downwind of major Asian source regions in spring 2004 (Chand et al., 2008)

483   and in the equatorial region in 2011 (Wang et al., 2014) (Table S2; references therein). The

484   maximum concentration from a decade of studies was 700 pg m^{-3} (3-h) measured in air masses

485   originated from upper air over the *Pacific* (Timonen et al., 2013), about two orders of magnitude

486   larger than what Chand et al. (2008) and Laurier et al. (2003) reported. PBM concentrations

487   over the *Pacific* reached up to 17 pg m^{-3}, comparable to GOM, and on average were three times

488   larger downwind of East Asia (3.0±2.5 pg m^{-3}) than in the equatorial *Pacific* MBL (Chand et al.,

489   2008; Wang et al., 2014) (Table S3).

490   In the southern *Indian* Ocean, very low GOM and PBM concentrations were observed,

491   averaged at 0.34 (<LOD (0.28 – 0.42 pg m^{-3}) – 4.07 pg m^{-3}) and 0.67 pg m^{-3} (<LOD – 12.67 pg

492   m^{-3}), respectively, over two years from a remote location, Amsterdam Island (Angot et al., 2014).

493   These concentrations were at the lower end of the range of *Atlantic* and the *Pacific* MBL

494   measurements.

495   Measurements over the *Mediterranean Sea* and its neighboring seas generally showed

496   much higher concentration levels than over the *Atlantic, Pacific*, and *Indian* Ocean, with GOM

497   ranging from 0.1 pg m^{-3} over the *Adriatic* (Sprovieri and Pirrone, 2008) to 4018 pg m^{-3} over the

498   *Dead Sea* (Obrist et al., 2011) (Tables S2 & S3; references therein). Frequency distributions of

499   24-hour average GOM and PBM concentrations from a site situated in the Mediterranean MBL

500   exhibited log-normal distributions with the maximum frequency at around 59 and 48 pg m^{-3},

501   respectively (Pirrone et al., 2003). One of the major findings from Sprovieri et al. (2003) was

502   constant presence of GOM averaged at 7.9±0.8 pg m^{-3} in the MBL over a 6000 km long cruise

503   path around the Mediterranean Sea. In a one year dataset of 2008, Beldowska et al. (2012)

504   showed 24-h PBM concentrations varied over 2 – 142 pg m^{-3} averaged at 20±18 pg m^{-3} with 93%

505   on average in the coarse fraction (>2 μm) over the southern *Baltic* Sea.

506   In springtime *Arctic*, the highest concentrations of GOM at 900 – 950 pg m^{-3} were

507   observed during the 1998 – 2001 Barrow Atmospheric Mercury Study (BAMS). Very high

508   springtime PBM concentrations (mean 394 pg m^{-3}, 47 – 900 pg m^{-3}, 1-h) were reported over

509   Beaufort Sea sea ice by Steffen et al. (2013). This was an order of magnitude higher than

510   concurrent GOM concentrations (mean 30 pg m^{-3}, 3.5 – 104.5 pg m^{-3}) and even larger than those

511   in temperate regions, where particle concentrations tended to be large. In comparison, Sommar et

512   al. (2010) found very low GOM and PBM over the summertime Arctic Ocean.

513   Over the *Antarctica*, 2-h GOM concentrations ranged over 10.5 – 334 pg m^{-3} averaged at

514   116.2±77.8 pg m^{-3} in Terra Nova Bay during spring – summer 2000 (Sprovieri et al., 2002), and

515   a similar range was also observed by Temme et al. (2003b) at the Neumayer Station in summer

516   2001 (Table S2). A range of 30 – 140 pg m^{-3} (80-min) was reported for peaks of GOM in

517   summer 2007 (Soerensen et al., 2010). Concentrations of 1-h PBM from Temme et al. (2003b)

518   varied over 15 – 120 pg m^{-3}, a range a factor of 3 smaller than that of concurrent GOM, tracking

519   GOM well only at a lower level. Different from the *Arctic*, summertime GOM concentrations

520   over the *Antarctic* were orders of magnitude larger.

521   2.2.2 Hemispheric Difference

522   Hemispheric gradient has been measured in both GOM and PBM since the early 1980s

523   (Slemr et al., 1985; Soerensen et al., 2010). In the first shipboard study by Slemr et al. (1985),

524   PBM concentrations of 0.013 ± 0.018 and 0.007 ± 0.004 ng m^{-3} over the North and South

525   *Atlantic* Ocean, respectively, were derived from Hg concentrations in rain water. About three

526   decades later Soerensen et al. (2010) reported hemispheric difference of GOM with a NH

527   average of 0.3 ± 3 pg m^{-3} in summer and 0.8 ± 2 pg m^{-3} in spring, and a seasonally invariable SH

528   average of 4.3 ± 0.14 pg m^{-3}.

529   2.2.3 Temporal Variations from Diurnal to Long-term Trend

530   2.2.3.1 Diurnal Variation

531   While some studies found a lack of diurnal variation in GOM (Sheu and Mason, 2001;

532   Aspmo et al., 2006; Temme et al., 2003b), many reported distinct diurnal variation with noon-

533   afternoon peaks and nighttime minimums in various oceanic regions (Mason et al., 2001; Mason

534   and Sheu, 2002; Lindberg et al., 2002; Laurier et al., 2003; Sprovieri et al., 2003, 2010; Laurier

535   and Mason, 2007; Mao et al., 2008; Chand et al., 2008; Sigler et al., 2009b; Soerensen et al.,

536   2010; Mao and Talbot, 2012; Wang et al., 2014). Over the *Atlantic* amplitude values varied from

537   0.27 pg m^{-3} in winter 2010 near the coast of southern New Hampshire, USA (Mao and Talbot,

538   2012) to >80 pg m^{-3} on the cruise from Barbados via Bermuda to Baltimore, Maryland, USA

539   (Mason and Sheu, 2002; Laurier and Mason, 2007). Over the *Pacific* amplitude values exceeded

540   80 pg m^{-3} (Laurier et al., 2003; Chand et al., 2008; Wang et al., 2014). Over the *Mediterranean*

541   Sea and its neighboring seas diurnal amplitude reached up to 35 pg m^{-3} (Sprovieri et al., 2003;

542   Sprovieri et al., 2010). The most pronounced diurnal variation was observed in the springtime

543   *Arctic* with noontime peaks up to 900 – 950 pg m^{-3} and near zero concentrations at night

544   (Lindberg et al., 2002).

545   The diurnal pattern of PBM concentrations, measured using a Tekran speciation unit, at a

546   midlatitude North *Atlantic* near coastal MBL site was in general not consistent between seasons

547   and years with seasonally averaged daily peaks 0.2 – 0.7 ppqv (1.7 – 6.2 pg m^{-3}) at varying time

548   of a day (Mao and Talbot, 2012).   The Tekran PBM instrument measures PBM on particles <

549   2.5 μm. Using a 10-stage impactor, Feddersen et al. (2012), perhaps the first to study the size

550   distribution of PBM in MBL, reported PBM concentrations (up to 0.25 ppqv, i.e. 2.2 pg m^{-3}, in

551   3.3 – 4.7 μm) in ten size fractions (<0.4 μm to >10 μm) at the same MBL location from Mao and

552   Talbot (2012), and found a diurnal cycle with daily maximums at around 16:00 UTC (noon local

553   time) and minimums around sunrise.

554   2.2.3.2 Seasonal to Annual Variation

555   Studies reported distinct seasonal variation in GOM with higher concentrations in

556   warmer months and lower in colder months (Mason et al., 2001; Mason and Sheu, 2002; Pirrone

557   et al., 2003; Laurier and Mason, 2007; Sigler et al., 2009a; Sprovieri et al., 2010; Soerensen et al.,

558   2010; Mao and Talbot, 2012; Obrist et al., 2011; Moore et al., 2013; Wang et al., 2014; Angot et

559   al., 2014). A fairly flat baseline with negligible annual variation in GOM was observed at a

560   midlatitude North *Atlantic* MBL site near southern New Hampshire, USA, in a three year dataset,

561   with more variability in higher mixing ratios and seasonal median values ranging from 0.03 ppqv

562   (~0.27 pg m^{-3}) in winter 2010 to 0.55 ppqv (~4.9 pg m^{-3}) in summer 2007 (Mao and Talbot,

563   2012). Over the *Mediterranean* the fall 2004 campaign experienced no production of GOM

564   whereas the summer 2005 one saw very high concentrations varying over 21 – 40 pg m^{-3}

565   (Sprovieri et al., 2010a). In the *Dead* Sea MBL, AMDEs resulting in 1-h GOM up to 700 pg m^{-3}

566   occurred[3]occurred more frequently in the summer than in winter (Obrist et al., 2011; Moore et al.,

567   2013).

568   In the *Arctic* MBL, several hundreds of pg m^{-3} GOM concentrations were observed in

569   spring (Lindberg et al., 2002; Steffen et al., 2013) and very low GOM and PBM concentrations

570   in summer (Sommar et al., 2010). Quite differently, summertime GOM concentrations over the

571   *Antarctic* seemed to be orders of magnitude larger (Sprovieri et al, 2002; Temme et al., 2003b;

572   Soerensen et al., 2010).

573   Some studies observed seasonal variation in PBM. Sprovieri et al. (2010a) found PBM

574   concentrations on average were more than a factor of 2 higher during high Hg episodes in the fall

575   than during the summertime ones over the *Mediterranean* Sea. Beldowska et al. (2012)

576   measured an average 24-h PBM of 15 pg m^{-3} and a 3 – 67 pg m^{-3} range in the non-heating season

577   compared to an average of 24 pg m^{-3} and a range of 2 – 142 pg m^{-3} in the heating season. The

578   PBM measurements at a *North Atlantic* coastal site using a 10-stage impactor showed distinct

579   seasonal variation with 50-60% of PBM in coarse fractions, 1.1 – 5.8 μm, composed largely of

580   sea salt aerosols at both sites in summer and 65% in fine fractions in winter (Feddersen et al.,

581   2012). Over the *Indian* Ocean significantly higher concentrations were observed in winter than

582   in summer (2.18±1.56 ng m^{-3} vs. 1.79±1.15 pg m^{-3}) (Angot et al., 2014).)

583   2.2.4 Mechanisms Driving the Observed Temporal Variabilities

584   2.2.4.1 Factors Causing Episodic High and Low Concentrations

585   Long range transport of air masses of terrestrial origin with high PBM concentrations was

586   evidenced in elevated crustal enrichment factors in the PBM samples (Lamborg et al., 1999).

587   An episode of high GOM concentrations coincided with a passing hurricane was linked to

588   downward mixing of air aloft with higher GOM (Prestbo, 1997; Mason and Sheu, 2002). Low

589   GOM concentrations were found to be concurrent with high humidity (e.g., fog) and rainfall but

590   highest concentrations on the day after such events if temperatures were elevated (Mason and

591   Sheu, 2002). High nighttime concentrations of GOM in the Mediterranean Basin were observed

592   in anthropogenic plumes identified using backward trajectories (Sprovieri et al., 2010a). The

593   GOM concentrations in air masses of marine origin at a site on the East Pacific coast were

594   unusually high ranging over $200 - 700$ pg m^{-3} (Timonen et al., 2013). The high GOM

595   concentrations were thought to be partitioned back from the PBM that was accumulated on

596   aqueous super-micron sea salt aerosols in the MBL when being lofted above the MBL, and an

597   anticorrelation between GOM and GEM was found in air masses of marine origin indicating

598   strong in-situ oxidation of GEM.

599   2.2.4.2 Diurnal Variation

600   The lack of GOM diurnal variation was speculated to result from diverse air masses with

601   different concentrations converging at the location leading to the removal of diurnal variation in

602   GOM (Sheu and Mason, 2001), and from low solar radiation (<200 W m^{-2}) at higher latitudes

603   (Aspmo et al., 2006). The majority of the studies reporting significant diurnal variation in GOM

604   attributed it to photooxidation, loss via dry deposition, and oceanic evasion, which was backed

605   up by modeling studies (Hedgecock et al., 2003, 2005; Laurier et al., 2003; Selin et al., 2007;

606   Strode et al., 2007).

607   It was generally found that GOM concentrations were positively correlated with solar

608   radiation flux and anticorrelated with relative humidity and at times with O_3 (Mason and Sheu,

609   2002; Laurier and Mason, 2007; Soerensen et al., 2010; Mao et al., 2012). The correlation

610   between GOM and UV radiation flux indicated photochemical processes, and the anticorrelation

611   between GOM and O_3 was caused by processes destroying O_3 and producing GOM (Mason and

612   Sheu, 2002; Laurier and Mason, 2007), especially the oxidation reactions in the presence of

27

613   deliquescent sea salt aerosols (Sheu and Mason, 2004).   The fact that GOM daytime peaks over

614   the *Pacific* increased with lower wind speeds and stronger UV radiation suggested that GOM

615   was produced in situ via photochemically driven oxidation (Laurier et al., 2003; Chand et al.,

616   2008). Chand et al. (2008) estimated the magnitude of GOM close to the amount produced from

617   the reaction of GEM + OH alone. Mao and Talbot (2012) suspected that unknown production

618   mechanism(s) of GOM in the nighttime MBL kept the levels above the LOD. Positive

619   correlation between GOM/PBM and temperature indicated possible temperature dependence of

620   certain oxidation reactions and gas-particle partitioning, whereas the anti-correlation between

621   GOM/PBM and wind speed indicated enhanced loss via deposition caused by faster wind speed

622   over water (Mao et al., 2012).

623   No consistent diurnal variation in PBM measured using a Tekran speciation unit

624   suggested more complicated processes than photochemistry involved in PBM budgets (Mao et

625   al., 2012). However, Feddersen et al. (2012) found diurnal variation in 10-stage impactor PBM

626   measurement data and speculated that GEM oxidation drove the PBM daytime maximum at

627   around 16:00 UTC (noon local time) and depositional loss at night without replenishment led to

628   the minimum around sunrise. In the same study, the large peaks of PBM appeared to be of

629   continental origin.

630   2.2.4.3 Seasonal to Annual Variation

631   Larger concentrations of GOM in spring and/or summer were generally associated with

632   stronger photo oxidation, biological activity, biomass burning, oceanic, and anthropogenic

633   emissions whereas low concentrations with wet deposition (Lindberg et al., 2002; Mason and

634   Sheu, 2002; Temme et al., 2003b; Pirrone et al., 2003; Sprovieri et al., 2003; Hedgecock et al.,

635   2004; Laurier and Mason, 2007; Sprovieri and Pirrone, 2008; Sprovieri et al., 2010; Soerensen et

636   al., 2010; Obrist et al., 2011; Mao et al., 2012; Angot et al., 2014; Wang et al., 2014). The

637   positive correlation between GOM concentration and solar radiation was used to explain warm

638   season maximums of GOM based on the same line of reasoning that was used to explain daytime

639   peaks of GOM (Mason and Sheu, 2002; Pirrone et al., 2003; Mao et al., 2012). Observed

640   seasonal variation in PBM was attributed to anthropogenic influence and gas-particle partitioning

641   as well as condensation and coagulation of fine particles (Sprovieri et al., 2010a; Beldowska et

642   al., 2012).

643   Over the *Mediterranean* Sea and its neighboring seas, it was generally thought that

644   meteorological conditions combined with anthropogenic, oceanic, and biomass emissions caused

645   GOM and PBM seasonal variation (e. g. Pirrone et al., 2003; Sprovieri et al., 2003; Hedgecock et

646   al., 2004; Sprovieri and Pirrone, 2008). A case in point is the seasonal contrast of no production

647   and little variation in GOM due likely to strong removal under the wet conditions in fall 2004

648   and very high concentrations due to strong oxidation under dry, sunny conditions in summer

649   2005 (Sprovieri et al., 2010). Sensitivity box model simulations suggested that the Hg + Br

650   controlled the production rate of GOM without contributions from the oxidation reactions by O_3

651   and OH and that HgBr was quickly converted to GOM. In the same study it was brought to

652   attention that biomass burning and ship emissions in the region were not included in the emission

653   inventory but could be important to ambient concentrations (Sprovieri et al., 2010). The authors

654   suggested that ship emissions could become a more important source of contaminants as

655   emissions from other sources were being more stringently controlled, and also the Mediterranean

656   was a place where busy shipping routes ran close to population centers. However, no studies

657   have demonstrated that ship emissions were an important source of Hg.

29

658   In the *Dead* Sea MBL, frequent occurrences of MDEs in the summer were linked to

659   higher BrO concentrations indicative of Br-initiated oxidation of GEM despite high temperature

660   and sometimes low BrO concentrations (Obrist et al., 2011). There is apparent discrepancy

661   between our theoretical understanding of the conditions required for Br-initiated GEM oxidation

662   and the real atmospheric conditions in the summertime Dead Sea MBL.

663   Wang et al. (2014) proposed iodine in a two-step mercury oxidation mechanism, where

664   BrHgI was hypothetically formed, helped to reconcile the modelled GOM with the observed

665   annual maximum GOM in October over the *equatorial Pacific*. The authors mentioned that HO_2

666   and/or NO_2 aggregation with HgBr from Dibble et al. (2012) could be another possibility and

667   further suggested that a major process in representing Hg oxidation is missing in current models.

668   Lindberg et al. (2002) found that springtime *Arctic* maximum concentrations of GOM at

669   900 – 950 pg m^{-3} corresponded to open leads over sea ice and an extensive area of elevated BrO

670   concentrations under the calmest conditions and strongest UV radiation. Low GOM and

671   unusually large PBM concentrations over Beaufort Sea sea ice in spring 2009 were speculated to

672   be caused by low temperatures and GOM formation followed by adsorption onto available sea

673   salt and sulfate aerosols, as well as ice crystals around the sea ice (Steffen et al., 2013). In

674   contrast, very low summertime Arctic GOM and PBM were due possibly to low in situ oxidation

675   of GEM and enhanced physical scavenging as a result of low visibility and high relative

676   humidity (Sommar et al., 2010).

677   Higher concentrations of GOM over the *Antarctic* Ocean were first proposed by Sprovieri

678   et al. (2002) to be produced from gas-phase oxidation of GEM by O_3, H_2O_2, and OH together

679   with favorable physical conditions such as PBL height. Temme et al. (2003b) found that the

680   highest concentrations of GOM corresponding to the lowest concentration of GEM falling below

681   the LOD (1.1 pg m^{-3}) during MDEs in summer were associated with the air masses having a

682   maximum contact with sea ice (coverage >40%) over the *South Atlantic* Ocean, which was

683   speculated to contain abundant reactive Br, released from sea salt associated with sea ice.

684   Summertime GOM was found to be correlated with GEM due probably to in situ oxidation and

685   build-up (Soerensen et al., 2010) and was also observed to be anti-correlated with GEM due

686   solely to oxidation (Temme et al., 2003b; Sprovieri et al., 2002).

687   **3. Continental Boundary Layer**

688   In this section, continental sites are defined as inland sites located in non-polar regions

689   and exclude locations impacted by the MBL, e.g. coastal sites and oceans.

690   ***3.1 TGM/GEM***

691   3.1.1 Concentration Metrics

692   Field measurements of TGM/GEM at continental sites were conducted mainly in Asia,

693   Canada, Europe, and USA. Very few TGM/GEM measurements have been made at inland sites

694   in the SH. Of all the four regions, the median concentrations of TGM or GEM were 1.6 ng m^{-3}

695   at remote and rural surface (low elevation) sites, 2.1 ng m^{-3} at urban surface sites, and 1.7 ng m^{-3}

696   at high elevation sites (**Fig. 2a**). TGM/GEM ranged over 0.1-11.3 ng m^{-3} at remote sites, 0.2-

697   18.7 ng m^{-3} at rural sites, 0.2-702 ng m^{-3} at urban sites, and 0.6-106 ng m^{-3} at high elevation sites.

698   Overall these statistics indicate that TGM/GEM at continental urban sites were higher and had

699   larger variability than rural and remote surface sites and high elevation sites in the NH. By

700   geographical region (**Fig. 2b**), the median TGM/GEM in Asia, comprising of sites

701   predominantly in China and a few sites in Korea and Japan, were higher by 26-55% than those in

702   Europe, Canada, and USA in this respective order. Although a higher median TGM/GEM was

703   found in Asia, the maximum single 5-min concentration was recorded in the USA (324 ng m^{-3},

704 Engle et al., 2010). The 5-min maximum TGM/GEM among the four regions was the lowest in

705 Europe (23 ng m^{-3}, Witt et al., 2010). It is important to note that most urban sites in the literature

706 are located in North America and Europe, and hence the higher TGM/GEM at continental urban

707 sites as shown in **Fig. 2b** were predominantly driven by measurements at those sites (instead of

708 Asian sites). A summary of the mean and the range of TGM/GEM as well as the distribution of

709 mean TGM/GEM at individual continental sites can be found in **Fig. S1** and Table S4. Statistics

710 from studies prior to 2009 are referred to in Sprovieri et al. (2010b).

711   3.1.2 Temporal Variations from Diurnal Cycle to Long-term Trends

712   3.1.2.1 Diurnal Variation

713 At *remote* surface locations, the diurnal variation of TGM/GEM is characterized by a daytime

714 increase reaching a maximum concentration in the afternoon and nighttime decrease

715 (Manolopoulos et al., 2007; Cheng et al., 2012). At *rural* surface and *high elevation* sites,

716 several different diurnal patterns have been reported. The first pattern, similar to remote surface

717 locations, is an early morning minimum, followed by midday to afternoon maximum and

718 decrease at night (Swartzendruber et al., 2006; Yatavelli et al., 2006; Choi et al., 2008, 2013; Fu

719 et al., 2008, 2009, 2010, 2012b; Lyman and Gustin, 2008; Mao et al., 2008; Obrist et al., 2008;

720 Faïn et al., 2009; Sigler et al., 2009; Mazur et al., 2009; Nair et al. 2012; Mao and Talbot, 2012;

721 Eckley et al., 2013; Parsons et al., 2013; Cole et al., 2014; Brown et al., 2015; Zhang et al., 2015).

722 The second diurnal pattern typically observed is a higher nighttime TGM/GEM than daytime.

723 This tends to occur in Asia and more polluted sites outside of Asia, e.g. abandoned Hg mines and

724 cement plants (Lyman and Gustin, 2008; Wan et al., 2009a; Rothenberg et al., 2010; Li et al.,

725 2011; Nguyen et al., 2011; Fu et al., 2012a; Gratz et al., 2013; Zhang et al., 2013; Cole et al.,

726 2014). The third pattern found at rural surface and elevated sites is a weak or lack of diurnal

727   pattern in TGM/GEM (Choi et al., 2008, 2013; Mao et al., 2008; Sigler et al., 2009; Engle et al.,

728   2010; Rothenberg et al., 2010; Mao and Talbot, 2012; Zhang et al., 2013; Han et al., 2014).

729   At *urban* surface sites, the predominant diurnal pattern is an increase in TGM/GEM

730   throughout the night that leads to a maximum in the early morning and a decrease in TGM/GEM

731   in the afternoon (Stamenkovic et al., 2007; Li et al., 2008; Choi et al., 2009; Lyman and Gustin,

732   2009; Song et al., 2009; Liu et al., 2010; Witt et al., 2010; Nguyen et al., 2011; Nair et al., 2012;

733   Zhu et al., 2012; Gratz et al., 2013; Kim et al., 2013; Civerolo et al. 2014; Cole et al., 2014; Han

734   et al., 2014; Lan et al., 2014; Xu et al., 2014; Xu et al., 2015). The diurnal amplitude tends to be

735   higher during summer compared to other seasons (Stamenkovic et al., 2007; Peterson et al. 2009;

736   Civerolo et al. 2014; Lan et al., 2014; Xu et al., 2014). Diurnal variations with daytime

737   maximum and early morning minimum have also been observed at *urban* surface sites (Fostier

738   and Michelazzo, 2006; Rothenberg et al., 2010; Witt et al., 2010; Jiang et al., 2013; Han et al.,

739   2014).

740   3.1.2.2 Seasonal Variation

741   The seasonal variation in TGM/GEM at some continental *remote* surface sites can be

742   characterized by a winter to early-spring maximum and lower summer/fall concentrations

743   (Manolopoulos et al., 2007; Cheng et al., 2012). At other *remote* sites, a completely opposite

744   seasonal pattern was found with higher summer/fall concentrations than winter/spring (Abbott et

745   al., 2008; Cole et al., 2014). The predominant seasonal TGM/GEM trend at *rural* surface and

746   *elevated* sites is the winter to spring maximum and summer/fall minimum (Zielonka et al., 2005;

747   Yatavelli et al., 2006; Choi et al., 2008; Fu et al., 2008, 2009, 2010; Mao et al., 2008; Sigler et al.,

748   2009a; Mazur et al., 2009; Engle et al., 2010; Mao and Talbot, 2012; Nair et al., 2012; Chen et

749   al., 2013; Parson et al., 2013; Cole et al., 2014; Marumoto et al., 2015). Other studies conducted

750   in *rural* sites and *elevated* sites found higher TGM/GEM during warm seasons (spring/summer)

751   than in the winter (Weiss-Penzias et al., 2007; Obrist et al., 2008; Nguyen et al., 2011; Eckley et

752   al., 2013; Zhang et al., 2013; Zhang et al., 2015).

753   The seasonal patterns at continental *urban* surface sites can be vastly different from each

754   other. Five major seasonal patterns have been identified including (1) a winter to spring

755   maximum (Fostier and Michelazzo, 2006; Stamenkovich et al. 2007; Choi et al., 2009; Peterson

756   et al., 2009; Civerolo et al., 2014; Xu et al., 2015), (2) a summer TGM/GEM maximum (Xu and

757   Akhtar, 2010; Jiang et al., 2013), (3) higher TGM during both winter and summer (Xu et al.,

758   2014), (4) higher TGM/GEM during spring/summer (Liu et al., 2007, 2010; Song et al., 2009;

759   Nair et al., 2012; Zhu et al., 2012; Hall et al., 2014), and (5) an absence of a clear seasonal trend

760   (Kim et al., 2013; Civerolo et al., 2014; Marumoto et al., 2015). Table 1 summarizes the

761   predominant diurnal and seasonal patterns observed at *rural, urban* and *high elevation*

762   continental sites.

763   3.1.2.3 Long-term Trends

764   At *rural* sites across Canada, TGM decreased at a rate of 0.9-3.3% per year between 1995

765   and 2011, which was determined using 5-15 years of TGM data depending on the location (Cole

766   et al., 2014). A GEM decrease of 0.056 ng m^{-3} yr^{-1} from 2005-2010 was found at an *elevated* site

767   in New Hampshire (Mao and Talbot, 2012). Widespread declines in GEM across North America

768   between 1997 and 2007 have also been reported (Weiss-Penzias et al., 2016); however, the

769   trends were not determined separately for rural and urban sites. No significant trends in TGM

770   were found at *urban/industrial* sites in the UK from 2003-2013 (Brown et al., 2015) and at

771   another urban site in Seoul, Korea from 2004-2011 (Kim et al., 2013). However, a short-term

772   annual TGM decrease from 2.0 to 1.7 ng m^{-3} was recorded at an urban site in Windsor, Canada

773   from 2007-2009 (Xu et al., 2014). At a chlor-alkali site in the UK, TGM declined by 1.36 ± 0.43

774   ng m^{-3} yr^{-1} from 2003-2012 (Brown et al., 2015). Weigelt et al. (2015) determined annual TGM

775   trends for different air masses arriving at Mace Head, Ireland between 1996 and 2013.

776   Specifically for continental airflows, TGM decreased by 0.0240 ± 0.0025 ng m^{-3} yr^{-1} for polluted

777   air masses from Europe, which was a slightly faster decline compared to marine airflows from

778   the North Atlantic Ocean (-0.0209 ± 0.0019 ng m^{-3} yr^{-1}) and the SH (-0.0161 ± 0.0020 ng m^{-3} yr^{-}

779   ^{1}). In certain months, the TGM decreases associated with local and European airflows (0.047-

780   0.051 ng m^{-3} yr^{-1}) were greater than other months (Weigelt et al., 2015).

781   3.1.3 Mechanisms Driving the Observed Temporal Variabilities

782   3.1.3.1 Diurnal Variation of TGM/GEM

783   TGM/GEM was higher during daytime than nighttime and often declined to a minimum

784   in the early morning at *remote, rural, high elevation*, and *some urban* surface sites (Table 1).

785   One of the mechanisms driving this diurnal pattern involved meteorological parameters, such as

786   temperature, the increase of which enhances TGM/GEM volatilization (Manolopoulos et al.,

787   2007; Mao et al., 2012; Jiang et al., 2013; Han et al., 2014). Surface emissions of TGM can

788   occur during daytime from soil and snow as temperature and solar radiation increases (Mao et al.,

789   2012; Cole et al. 2014). Solar radiation minimizes the activation energy required for Hg

790   emissions (Zhu et al., 2012) and increases Hg photoreduction in soil and snow (Steffen et al.,

791   2008; Zhu et al., 2012; Hall et al., 2014; Xu et al., 2014; Xu et al., 2015). This process appeared

792   to be especially relevant at sites with elevated Hg in soil (Lyman and Gustin, 2008; Brown et al.,

793   2015) because of a larger flux gradient. Dry deposition of GEM in the night might also played a

794   role since deposition was typically observed in nighttime in contrast to emission during daytime

795   (Zhang et al., 2009). Fog or dew formation occurring in the late summer was believed to have

796 caused GEM depletion in the early morning hours by capturing GEM in fog or dew water

797 (Manolopoulos et al., 2007; Mao and Talbot, 2012). Another driving mechanism of this

798 TGM/GEM diurnal pattern was the change in the boundary layer mixing height. Lower

799 TGM/GEM during nighttime is due to TGM/GEM deposition as the nocturnal inversion layer

800 forms. In the morning, the nocturnal inversion breaks down and mixes with TGM/GEM-rich air

801 in the residual layer and subsequently leads to increasing TGM/GEM during the day (Yatavelli et

802 al., 2006; Mao et al., 2008; Mazur et al., 2009; Mao and Talbot, 2012; Nair et al. 2012; Choi et

803 al., 2008, 2013; Jiang et al., 2013; Cole et al., 2014). At *elevated* sites, there was a transition

804 from the sampling of boundary layer during daytime to free troposphere air at night which was

805 driven by mountain/valley atmospheric patterns (Obrist et al., 2008). During daytime, mountain

806 breeze causes moist air to ascended from the surface to higher altitudes carrying with it GEM

807 from the boundary layer (Swartzendruber et al., 2006; Obrist et al., 2008; Fu et al., 2010, 2012b;

808 Zhang et al., 2015). At night, drier free troposphere air impacted the elevated site leading to

809 lower GEM and water vapor and higher GOM and ozone (Obrist et al., 2008). A lack of diurnal

810 variability was also reported at some rural surface locations, although the driving mechanism is

811 not quite clear. At an elevated site, the sampling of air above the nocturnal boundary layer and

812 lack of anthropogenic sources or GEM oxidants near the site led to constant GEM during most of

813 the time except in the summer (Mao et al., 2008; Sigler et al., 2009a; Mao and Talbot, 2012).

814 Thus this differed from other mountain sites, which were affected by surface emissions and

815 local/regional transport of GEM from the boundary layer during daytime.

816   At most *urban* sites and some *elevated* and polluted rural sites, the nighttime TGM

817 concentrations were higher than daytime, and the maximum concentration typically occurred in

818 the early morning before sunrise (Table 1). This type of diurnal variation was driven by

819   nighttime accumulation of TGM/GEM near the surface due to a shallow nocturnal boundary

820   layer and dilution during the day initiated by convective mixing with cleaner air aloft as the

821   mixing layer increases (Stamenkovic et al., 2007; Li et al., 2008; Lyman and Gustin, 2008, 2009;

822   Choi et al., 2009; Wan et al., 2009a; Rothenberg et al., 2010; Witt et al., 2010; Li et al., 2011;

823   Nguyen et al., 2011; Fu et al., 2012a; Nair et al., 2012; Zhu et al., 2012; Gratz et al., 2013; Kim

824   et al., 2013; Zhang et al., 2013; Cole et al., 2014; Lan et al., 2014; Xu et al., 2014). The shallow

825   nocturnal boundary layer was often associated with high TGM coinciding with low wind speeds

826   at night (Li et al., 2008; Fu et al., 2012a; Lan et al., 2014). Increases in nighttime concentrations

827   could also be driven by nighttime sources, such as emissions from mercury mining regions

828   (Lyman and Gustin, 2008) and local emissions occurring at night (Song et al., 2009; Wan et al.,

829   2009a; Rothenberg et al., 2010; Gratz et al., 2013; Kim et al., 2013). At *urban* surface sites,

830   studies suggested the driving mechanisms for the morning maximum were surface emissions

831   (Zhu et al., 2012; Hall et al., 2014; Xu et al., 2014; Xu et al., 2015), volatilization of Hg from

832   dew (Zhu et al., 2012), and vehicular traffic emissions evident by correlations between

833   TGM/GEM and CO and NO_x (Zhu et al., 2012; Xu et al., 2015). However, there is little research

834   suggesting significant amounts of Hg from vehicular emissions (Conaway et al., 2005; Landis et

835   al., 2007; Won et al., 2007). The general view is that the global contribution from petroleum

836   fuels combustion represented 0.00013% of the total anthropogenic emissions and thus can be

837   neglected in global assessment of Hg emissions (Pirrone et al., 2010). The lower TGM/GEM

838   observed in the afternoon was driven by GEM oxidation (Stamenkovic et al., 2007; Choi et al.,

839   2009; Lyman and Gustin, 2009; Li et al., 2011; Nguyen et al., 2011; Kim et al., 2013; Zhang et

840   al., 2013; Xu et al., 2014; Xu et al., 2015).

841   Many studies conducted in *urban* areas found a larger diurnal amplitude during summer

842   than other seasons. The major driving mechanism for this larger amplitude originated from

843   higher solar radiation and temperature, which increased the boundary layer mixing height in the

844   summer (Civerolo et al., 2014; Xu et al., 2014). Higher solar radiation during summer also

845   increased photochemical reactions, like GEM oxidation. The larger diurnal variation was also

846   attributed to increases in uptake and re-emissions by vegetation and power plant emissions from

847   air conditioner use during summer nights (Xu et al., 2014). The shift in the timing of the

848   TGM/GEM maximum varied with season at some urban sites. During spring in Windsor,

849   Canada, the decrease in TGM earlier in the afternoon was thought to be due to increase

850   photochemical processes resulting from higher solar radiation and lower GEM emissions due to

851   less vegetation coverage in the spring (Xu et al., 2014). In Nanjing, China, the peak

852   concentration occurring later in the morning during spring was driven by prolonged sunlight

853   hours (Zhu et al., 2012).

854   Site characteristics may have different impacts on the diurnal variation. During nighttime,

855   GEM at an *urban* site was significantly higher than a rural site suggesting higher GEM fluxes

856   from buildings and pavement than vegetation and soil (Liu et al., 2010), but may be simply

857   caused by stronger and more anthropogenic sources in urban areas. The diurnal amplitude at an

858   *urban* site was greater than a suburban site in one study; however, the reason was not known

859   (Civerolo et al., 2014). In the same study, nighttime GEM was 25-30% higher than daytime for

860   the urban site close to the Atlantic Ocean, whereas the GEM difference between night and day

861   was only 10% at an inland suburban site (Civerolo et al., 2014). The study suggested that the

862   higher halogen concentrations in marine environments increased GEM oxidation and

863   subsequently, the loss of GEM in the afternoon leading to larger diurnal variation. At a different

864 coastal-urban location, nighttime GEM was only slightly higher than daytime because of the

865 cleaner air transported from the marine environment (Nguyen et al., 2011). These studies

866 suggested that MBL influence could lead to very different diurnal patterns. Sites continuously

867 impacted by Hg point sources likely contributed to the large short-term fluctuations in the diurnal

868 patterns at some urban sites (Rutter et al., 2008; Engle et al., 2010; Witt et al., 2010).

869   3.1.3.2 Seasonal Variation of TGM/GEM

870   The seasonal variation exhibiting a winter to spring maximum in remote, rural, urban and

871 high elevation environments (Table 1) was suggested to be driven by multiple mechanisms,

872 including anthropogenic emissions for winter heating (coal and wood combustion), reduced

873 atmospheric mixing, decreased GEM oxidation, less scavenging, and emissions from soil,

874 vegetation, and melting snow in the spring (Stamenkovic et al., 2007; Choi et al., 2008; Mao et

875 al., 2008; Sigler et al., 2009a; Peterson et al., 2009; Wan et al., 2009a; Cheng et al., 2012; Mao

876 and Talbot, 2012; Civerolo et al., 2014; Cole et al., 2014; Xu et al., 2015). The lower

877 TGM/GEM during summer has been attributed to increased GEM oxidation, uptake by

878 vegetation, and higher wet deposition of GOM (Yatavelli et al., 2006; Fu et al., 2008, 2009;

879 Engle et al., 2010; Xu et al., 2015). While these were the predominant driving mechanisms of

880 the seasonal variations in the NH, the seasonal patterns could also be influenced by changes in

881 the prevailing wind patterns (Fostier and Michelazzo, 2006; Fu et al., 2010, 2015; Sheu et al.,

882 2010; Chen et al., 2013; Zhang et al., 2013; Hall et al., 2014). The impact of combustion

883 emissions from winter heating was ruled out at a subtropical site in the Pearl River Delta region

884 of China; instead, the elevated TGM in the spring was attributed to monsoons which advected

885 southerly marine air masses during summer and northeasterly winds from Siberia during winter

886 (Chen et al., 2013). The transition from cold dry air to warm moist air often led to strong

887   temperature inversion and haze in the spring, which in turn inhibits pollutant dispersion.

888   Summer and spring maxima in TGM/GEM have also been found at remote, rural, and urban

889   atmospheres. This pattern was predominantly driven by meteorology. Higher solar radiation

890   and temperature during summer increased GEM emissions from Hg contaminated soil (Zhu et al.,

891   2012; Eckley et al., 2013), from vegetation at a forested agricultural site (Nguyen et al., 2011),

892   and from urban surfaces such as soil and pavement in Windsor, Canada (Xu and Akhtar, 2010).

893   3.1.3.3 Long-term Trends of TGM/GEM

894   Long-term trends of TGM/GEM over continental regions indicated a declining trend at

895   some sites and no significant trend at others, particularly at urban sites. Previous studies partly

896   attributed the long-term TGM trends to anthropogenic Hg emissions reductions. There has been

897   a 60-70% decrease in anthropogenic Hg emissions from USA and Canada; however only up to

898   15% of those emissions reductions impacted TGM at Canadian sites (Cole et al., 2014). The

899   more rapid decline in TGM measured at Mace Head, Ireland for local and European air masses

900   compared to marine air masses was thought to be driven by Hg emissions reductions in Europe

901   (Weigelt et al., 2015). The baseline TGM at Mace Head decreased at a larger rate in November

902   than other months suggesting that it is related to lower Hg emissions from residential heating in

903   Europe. The 21% decline in TGM from 2006-2012 in urban/industrial areas of the UK was also

904   consistent with the 0.21 Mg yr^{-1} (24%) reduction in Hg emissions from the UK, even though the

905   TGM trend from the 2003-2013 period was not statistically significant (Brown et al., 2015). In

906   Seoul, Korea, no significant trend in TGM was found from 2004-2011, consistent with the slight

907   decrease (1%) in coal consumption in Seoul over the same time frame (Kim et al., 2013). While

908   TGM/GEM trends appear to be aligned with local/regional Hg emission trends, a discrepancy

909   exists when the trend was compared to the increasing global anthropogenic Hg emissions

910   (Sprovieri et al., 2010b; Ebinghaus et al., 2011; Cole et al., 2014). Alternative reasons for the

911   decline in TGM could be due to faster cycling of Hg as O_3 and other oxidants have been

912   increasing or lower emissions of previously-deposited Hg (Sprovieri et al., 2010b; Ebinghaus et

913   al., 2011). Modeling studies indicated global Hg emissions inventory have not accounted for the

914   changes in Hg speciation emission profiles from coal combustion and reduced emissions from

915   products containing Hg (Zhang et al., 2016).

916   *3.2 GOM and PBM*

917   3.2.1 Concentration Metrics

918   The highest median GOM and PBM were found at *high elevation* sites, while the lowest

919   concentrations were found at *rural* surface sites. The median GOM from all locations were 12.1

920   pg m^{-3} at *elevated* sites, 9.9 pg m^{-3} at *urban* sites, 3.8 pg m^{-3} at *remote* sites, and 2.8 pg m^{-3} at

921   *rural* sites (Fig. 2a), and correspondingly the median PBM concentration was 11.0, 10.0, 6.9, and

922   4.6 pg m^{-3}. The variabilities in GOM and PBM were greatest at urban locations. 2-3 hour GOM

923   concentrations ranged from <LOD-880 pg m^{-3} at elevated sites, <LOD-8160 pg m^{-3} at urban sites,

924   <LOD-224 pg m^{-3} at remote sites, and <LOD-462 pg m^{-3} at rural sites (see individual site

925   statistics and the map of mean concentrations at all sites in **Fig. S1** and Table S5). 2-3 hour

926   PBM concentrations ranged from <LOD-1001 pg m^{-3} at elevated sites, <LOD-11600 pg m^{-3} at

927   urban sites, <LOD-404 pg m^{-3} at remote sites, and <LOD-205 pg m^{-3} at rural sites (Table S6).

928   By geographical region, the median GOM in Asia was a factor of 1.4-5.1 higher than those in

929   Canada and USA (Fig. 2b). Similarly, the median PBM in Asia was 1.8-8.1 times higher than

930   those in Canada, Europe and USA. This was potentially because one-third of the elevated sites

931   were in China. The GOM and PBM maxima of 8160 pg m^{-3} and 11600 pg m^{-3}, respectively,

932   were both observed at an urban site in Illinois, USA (Engle et al., 2010; Table S5 and S6).

933	3.2.2 Temporal Variations from Diurnal Cycle to Seasonal Trends

934	3.2.1.1 Diurnal Variation

935	The predominant diurnal pattern of GOM at *remote, rural, urban,* and *elevated* sites was

936	an increase in the morning leading to a maximum sometime between midday to late afternoon

937	and eventually decreasing at night (Yatavelli et al., 2006; Manolopoulos et al. 2007; Abbott et al.,

938	2008; Lyman and Gustin, 2008; Faïn et al., 2009; Rothenberg et al., 2010; Cheng et al., 2012; Fu

939	et al., 2012a; Nair et al., 2012; Eckley et al., 2013; Gratz et al., 2013; Cole et al., 2014; Civerolo

940	et al., 2014; Marumoto et al. 2015; Zhang et al., 2015). Late evening increases in GOM were

941	observed at some *urban* and *elevated* sites (Lynam and Keeler, 2005; Song et al., 2009; Gratz et

942	al., 2013). The average GOM was 18-60 pg m^{-3} between midnight and early morning at two

943	*elevated* sites, whereas the average daytime GOM was 9.2-39 pg m^{-3} (Swartzendruber et al.,

944	2006; Sheu et al., 2010).

945	No predominant diurnal pattern was found for PBM, which was mostly measured using

946	the Tekran speciation unit (2537-1135-1130). At *rural* and *urban* sites, the types of diurnal

947	patterns include, daytime/afternoon peak (Yatavelli et al., 2006; Choi et al., 2008; Rothenberg et

948	al. 2010; Cole et al., 2014), increasing during daytime leading to a nighttime peak (Nair et al.,

949	2012; Zhang et al., 2013), or lack of variation (Cobbett and Van Heyst, 2007; Choi et al., 2008;

950	Rothenberg et al., 2010; Cole et al., 2014).

951	3.2.1.2 Seasonal Variation

952	No predominant seasonal pattern in GOM was found at *remote, rural, urban,* and

953	*elevated* sites. At *remote* sites, some studies observed a winter to early-spring maximum and

954	lower concentrations during summer/fall (Manolopoulos et al., 2007; Cheng et al., 2012),

955	whereas higher summer/fall than winter/spring concentrations were also reported (Abbott et al.,

956   2008). In *rural* and *elevated* sites, the maximum concentration occurred in different seasons. At

957   *urban* sites, the maximum GOM typically occurred in warmer seasons, e.g. spring or summer

958   (Song et al., 2009; Liu et al., 2010; Choi et al., 2013; Wang et al., 2013; Gratz et al., 2013;

959   Civerolo et al., 2014; Han et al., 2014; Marumoto et al., 2015; Xu et al., 2015). Higher PBM and

960   total particulate Hg (TPM) during colder seasons than summer was a highly ubiquitous trend for

961   *remote, rural, urban,* and *elevated* sites (Zielonka et al, 2005; Choi et al., 2008; Wan et al.,

962   2009b; Liu et al., 2010; Kim et al., 2012; Gratz et al., 2013; Beldowska et al., 2012; Marumoto et

963   al., 2015; Schleicher et al., 2015; Zhang et al., 2015). However, increases in PBM also occurred

964   during summer in a few studies (Song et al., 2009; Huang et al., 2010; Cheng et al., 2012).

965   3.2.3 Mechanisms Driving the Observed Temporal Variabilities

966   3.2.3.1 Diurnal Variations of GOM and PBM

967   The widespread observation of a midday to late afternoon peak in GOM at continental

968   sites (Table 1) often coincided with meteorological parameters, such as solar radiation and

969   temperature, and/or ozone (Yatavelli et al., 2006; Abbott et al., 2008; Wan et al., 2009a; Weiss-

970   Penzias et al., 2009; Nair et al., 2012; Mao et al., 2012; Gratz et al., 2013; Zhang et al., 2013;

971   Civerolo et al., 2014; Cole et al., 2014; Marumoto et al., 2015). At *high elevation* sites, GOM

972   was also inversely correlated with relative humidity, water vapor, or dew point temperature

973   (Swartzendruber et al., 2006; Lyman and Gustin, 2008, 2009; Weiss-Penzias et al., 2009), and in

974   some cases GOM was not correlated with O_3 (Lyman and Gustin, 2009; Peterson et al., 2009; Xu

975   et al., 2015). These diurnal trends indicated daytime *in-situ* photochemical production of GOM

976   or entrainment of GOM from the free troposphere due to convective mixing. Increases in GOM

977   during daytime at a rural site was attributed to local transport from urban areas as indicated by

978   similarities in diurnal patterns between GOM, SO_2, and O_3 and a delay in the timing of the GOM

979   maximum likely resulting from emissions transport (Rothenberg et al., 2010). Short-term

980   fluctuations in the diurnal pattern of GOM also suggested the influence of point sources (Rutter

981   et al., 2008; Engle et al., 2010). Dry deposition and scavenging of GOM by dew played a role in

982   decreasing GOM during nighttime (Liu et al., 2007; Wan et al., 2009b; Weiss-Penzias et al.,

983   2009; Nair et al., 2012; Choi et al., 2013; Civerolo et al., 2014). The stronger diurnal amplitude

984   during the spring/summer coincided with stronger correlations between GOM, solar radiation,

985   temperature and O_3 (Yatavelli et al., 2006; Mao et al., 2012; Gratz et al., 2013; Zhang et al.,

986   2013), which suggested that increased photochemical processes led to higher GOM. Large

987   diurnal variation during summer was also potentially driven by high pressure, drier and cloud-

988   free conditions that are conducive to the buildup of GOM in the free troposphere (Lyman and

989   Gustin, 2009).

990   Nighttime increases in GOM seen exclusively at *urban* and *elevated* sites (Table 1)

991   appeared to be driven by anthropogenic emissions and the free troposphere. Nocturnal emissions

992   and local/regional transport within the boundary layer (Lynam and Keeler, 2005; Song et al.,

993   2009) and reduced vertical mixing in the stable nocturnal boundary layer led to higher GOM at

994   night in *urban* areas (Gratz et al., 2013). At *high elevation* sites, katabatic winds entrained GOM

995   from the free troposphere. In one study, GOM from the free troposphere was believed to

996   originate from *in-situ* photochemical processes due to a strong inverse GEM-GOM correlation

997   and a GOM/GEM slope near unity during an elevated GOM episode (Swartzendruber et al.,

998   2006). While an anti-correlation between GEM and GOM was also found at another elevated

999   site, Sheu et al. (2010) did not observe a complete photochemical conversion of GEM to GOM.

1000   The difference between these two *elevated* sites suggested different sources of GOM in the free

1001   troposphere. Timonen et al. (2013) found that in one type of free troposphere air mass, GEM

1002   oxidation occurred in anthropogenic plumes transported from Asia to Mt. Bachelor Observatory,

1003   USA and converted 20% of the GEM to GOM. A second type of air mass travelling over the

1004   Pacific Ocean resulted in 100% GEM conversion to GOM likely because of GEM oxidation by

1005   bromine.

1006   The driving mechanisms behind the diurnal pattern of PBM were better explored for

1007   *urban* sites than other site categories. Frequent spikes in hourly concentrations during daytime

1008   were attributed to point sources (Rutter et al., 2008; Civerolo et al., 2014). At a valley *urban* site,

1009   higher PBM and GEM during daytime suggested similar emission sources from Hg enriched

1010   areas (Lyman and Gustin, 2009). Higher PBM during daytime in the summer could also be

1011   initiated by photochemical production of GOM followed by absorption on secondary organic

1012   aerosols (Choi et al., 2013). Diurnal patterns exhibiting nighttime increases in PBM in urban

1013   areas could be due to multiple mechanisms and sources, such as nocturnal emissions and

1014   local/regional transport within the boundary layer (Song et al., 2009), reduced vertical mixing in

1015   the stable nocturnal boundary layer (Gratz et al., 2013; Xu et al., 2015), vehicular emissions in

1016   China (Xu et al., 2015), and nighttime street food vending in Beijing (Schleicher et al. 2015).

1017   3.2.3.2 Seasonal Variations of GOM and PBM

1018   The seasonal variation characterized by higher GOM in the warm seasons (Table 1) was

1019   primarily driven by photochemical production due to increased solar radiation, O_3, and likely

1020   other atmospheric oxidants (Liu et al., 2010; Choi et al., 2013; Civerolo et al., 2014; Xu et al.,

1021   2015). Alternative reasons could be attributed to anthropogenic emissions leading to higher

1022   GOM in the summer at *urban* sites (Song et al., 2009; Gratz et al., 2013). Atmospheric mercury

1023   depletion events occurring at *higher latitude* continental sites led to higher GOM during spring

1024   (Cole et al., 2014). Free troposphere transport was a major driving mechanism for higher

1025   reactive Hg at three *high elevation* western U.S. sites (Weiss-Penzias et al., 2015). At *elevated*

1026   sites in China, the occurrence of higher GOM between fall and spring were attributed to coal and

1027   biofuel burning (Wan et al., 2009b) and changes in the prevailing winds that advected GOM

1028   from polluted regions (Fu et al., 2012a; Zhang et al., 2015). Lower GOM during summer was

1029   due to wet deposition (Wan et al., 2009b; Sheu et al., 2010).

1030   Several mechanisms contributed to the increase in PBM or TPM during colder seasons

1031   (Table 1) including, local/regional coal combustion and wood burning emissions, lower mixing

1032   height, less oxidation, and increased gas-particle partitioning (Song et al., 2009; Xiu et al., 2009;

1033   Liu et al., 2010; Cheng et al., 2012; Fu et al., 2012a; Kim et al., 2012; Choi et al., 2013; Gratz et

1034   al., 2013; Wang et al., 2013; Civerolo et al., 2014; Cole et al., 2014; Schleicher et al., 2015; Xu

1035   et al., 2015). Oxidized Hg tended to partition to particles during colder seasons because of lower

1036   temperatures (Rutter et al., 2007), higher relative humidity (Kim et al., 2012), and reduced

1037   volatilization of gaseous Hg (Choi et al., 2013). Similar to GOM, decreases in PBM during

1038   summer at many sites in China were due to wet deposition (Wan et al., 2009b; Schleicher et al.,

1039   2015; Xu et al., 2015; Zhang et al., 2015) and a shift to cleaner marine airflows during summer

1040   (Kim et al., 2012). Higher PBM during warm seasons may be driven by forest fire emissions

1041   (Eckley et al., 2013) and increased $PM_{2.5}$ available for GOM absorption at urban sites (Song et

1042   al., 2009; Schleicher et al., 2015).

1043   **4. Latitudinal Variation**

1044   There are a few shipboard and airborne studies that surveyed latitudinal variation of

1045   TGM/GEM (Slemr et al., 1981, 1985, 1995; Slemr and Langer, 1992; Fitzgerald et al., 1984;

1046   Lamborg et al., 1999; Temme et al., 2003a; Aspmo et al., 2006; Soerensen et al., 2010). Bagnato

1047   et al. (2013) compiled a latitudinal distribution of TGM/GEM using measurement data from a

1048　　number of shipboard measurement studies spanning the time period of 1980 – 2012 (**Fig. 3**) and

1049　　showed a small but discernible inter-hemispheric gradient, with the highest concentrations (~3.5

1050　　ng m^{-3}) in NH midlatitudes and the lowest in SH latitudes (~0.9 ng m^{-3}), resulting from greater

1051　　emissions of Hg in the more industrialized NH.

1052　　　　　Tropospheric airborne measurements from INTEX-B (Talbot et al., 2007, 2008) and

1053　　ARCTAS (Mao et al., 2010), spanning near the surface to 12 km altitude, suggested distinct

1054　　seasonal variation in GEM concentrations and latitudinal gradient. On average there was an

1055　　increase of ~50 ppqv (~0.5 ng m^{-3}) from lower latitudes (~20 – 30 °N) to higher (60 – 90°N)

1056　　latitudes in spring while negligible latitudinal variation in summer (**Fig. 4**). It was speculated

1057　　that smaller latitudinal gradient of temperature in summer likely enhanced meridional circulation

1058　　resulting in smaller latitudinal variation in GEM concentration in the troposphere.

1059　　　　　A small gradient was measured in atmospheric GEM concentrations over the *Pacific*

1060　　from 1.32 ng m^{-3} in 14 – 20°N latitudes to 1.15 ng m^{-3} in 1-15°S latitudes in October 2011

1061　　(Soerensen et al., 2014). Atmospheric GEM elevated in the northern part of the ITCZ was

1062　　temporarily influenced by the northeastern trade wind that enhanced oceanic evasion, consistent

1063　　with the largest evasion flux in that region.

1064　　**5. Altitude Variation**

1065　　　　　Airborne measurements of TGM, GEM, and/or GOM have been conducted since 1977

1066　　(Seiler et al., 1980) extending from near the surface to ~12 km altitude at several geographic

1067　　locations (Table S7; references therein). More recent studies showed GEM concentrations

1068　　remaining nearly constant *vertically*, slightly decreasing with altitude (Banic et al., 2003; Radke

1069　　et al., 2007; Talbot et al., 2007, 2008; Mao et al., 2010). *Seasonal variation* was observed from

1070　　surface to 7 km over Canada with ~1.5 ng m^{-3} in summer, 1.7 ng m^{-3} in winter, 1.7 ng m^{-3} >1 km

1071   altitude and 1.2 ng m^{-3} below 1 km due to widespread MDEs over the sea ice in the springtime

1072   Arctic (Banic et al., 2003). During ARCTAS, Mao at el. (2010) found that the vertical extent of

1073   springtime Arctic MDEs varied from meters to 1 km depending on the thickness of the surface

1074   inversion layer.

1075   Observation of low GEM in stratospherically influenced air led to the hypothesis that the

1076   upper troposphere/lower stratosphere (UTLS) was a Hg sink region (Radke et al., 2007). With

1077   repeated measurements of depleted GEM in stratospherically influenced air coupled with

1078   Murphy et al. (1998, 2006)'s findings of enrichment of PBM in lower stratospheric aerosols,

1079   Talbot et al. (2007) hypothesized that stratospheric GEM depletion was caused by fast oxidation

1080   of GEM by abundant halogen radicals and O$_3$ and estimated a lifetime of 2 and 0.5 days for 100

1081   ppqv GEM oxidized by O$_3$ and Br, respectively. Talbot et al. (2007) suggested that stratospheric

1082   intrusion could be a source of tropospheric Hg if PBM was to be transformed back to gaseous Hg.

1083   A 1 – 2 ng m^{-3} range of upper tropospheric GEM was reported by Ebinghaus et al. (2007)

1084   and elevated GEM concentrations in biomass burning plumes from the same study suggested

1085   biomass burning representing a major mercury source. In the atmosphere of East Asia, Friedli et

1086   al. (2004) was the first to report GEM concentrations from sea level to ~7 km altitude under the

1087   influence of continental export from East China, showing concentrations at all altitudes higher

1088   than the global background, with the largest 6.3 ng m^{-3} in an industrial plume mostly from coal

1089   combustion and at times from other sources including dust storms, biomass burning, and

1090   volcanic eruption. On a relevant note, Swartzendruber et al. (2008) suggested that long range

1091   transport of Asian pollution contributed to the higher GEM concentrations above 2.5 km, which

1092   increased with altitude from 1.30±0.084 ng m^{-3} in 0 – 0.5 km altitude to 1.52±0.182 ng m^{-3} in the

1093   highest layer 5.5 – 6.5 km altitude over the Pacific Northwest over 13 April – 16 May 2006.

1094   Upper air GOM concentrations were first measured in spring by Lindberg et al. (2002) at

1095   1000 m and 100 m altitude immediately northeast of Point Barrow. Six aircraft surveys

1096   consistently showed that GOM concentrations decreased from an average of 70 to 20 to 2 pg m^{-3}

1097   from 5 to 100 to 1000 m altitude, supporting the hypothesis that the Hg oxidation reactions

1098   occurred in the near-surface boundary layer driven by halogen compounds derived from sea-salt

1099   aerosols. In recent years, more studies attributed higher GOM concentrations in higher altitudes

1100   to lack of depositional loss, lower temperature, and/or more abundant Br radicals (Sillman et al.,

1101   2007; Lyman and Jaffe, 2011; Brooks et al., 2014; Gratz et al., 2015; Shah et al., 2016). Sillman

1102   et al. (2007) reported GOM concentrations measured in Florida increasing with height from 10 to

1103   230 pg m^{-3}, which was reproduced using CMAQ model (Bullock and Brehme, 2002) with gas-

1104   phase oxidation reactions GEM+O_3 and GEM+OH, the latter being dominant. Lyman and Jaffe

1105   (2011) found enhanced GOM concentrations of ~450 pg m^{-3} and depleted GEM in one

1106   stratospheric intrusion case and further speculated that the stratosphere was depleted in total Hg

1107   and enriched in GOM, and suggested that stratospheric intrusion could be a source of GOM to

1108   the troposphere. Near Tullahoma, TN, USA the highest GOM concentrations (200 – 500 pg m^{-3})

1109   from flights over a year were observed always at 2 – 4.5 km altitude with a strong *seasonal*

1110   *variation* with a wintertime minimum and a summertime maximum (Brooks et al., 2014). In the

1111   same study, limited PBM measurements exhibited similar levels to GOM at all altitudes.

1112   In a most recent field campaign NOMADSS, the highest Hg(II) concentrations of 300–

1113   680 pg m^{-3} were observed in dry (RH<35 %) and clean air masses during two flights over Texas

1114   at 5–7 km altitude and off the North Carolina coast at 1–3 km altitude (Gratz et al., 2015; Shah et

1115   al., 2016). Gratz et al. (2015) found, using back trajectories, that a segment of air masses with

1116   elevated GOM averaged at 0.266±0.038 ng m^{-3} and ranging over 0.182 – 0.347 ng m^{-3} at 7 km

1117   altitude over Texas originated from the upper troposphere of the Pacific High. It was speculated

1118   that the stable, dry conditions of large scale anticyclones resulted in a lack of GOM removal by

1119   wet deposition or in-cloud reduction and were thus ideal for GOM accumulation.   They

1120   demonstrated that elevated BrOx could persist and that sufficient GOM could be produced

1121   during long-range transport in the Pacific upper troposphere. Their sensitivity analysis suggested

1122   a range of 8 – 13 days required to produce the observed GOM. Shah et al. (2016), using the

1123   GEOS-Chem model with tripled bromine radical concentrations or a faster oxidation rate

1124   constant for GEM + Br, increased modeled Hg(II) concentrations by a factor of 1.5 – 2

1125   improving agreement with the observations, and suggested that the subtropical anticyclones were

1126   significant global sources of Hg(II).

1127   **6. Summary and Recommendations**

1128   This review summarized the general characteristics in GEM, GOM, and PBM

1129   concentrations in the MBL, over land, from low to high latitudes, and from the surface to the

1130   upper troposphere, and further the factors driving such variabilities based on a great wealth of

1131   research in the literature. The Key points are summarized below.

1132   1. For MBL TGM/GEM, diurnal variation in most oceanic regions featured noon to

1133   afternoon minimums due probably to in situ oxidation of GEM, while a few

1134   studies showed the opposite pattern over the *Atlantic* and the *equatorial Pacific*

1135   Ocean, attributed to enhanced oceanic evasion linked to enhanced photoreduction

1136   and biological activity. Seasonal to annual variation was generally characterized

1137   as higher (lower) concentrations in colder (warmer) months, which was largely

1138   thought to be caused by less (more) loss via oxidation in colder (warmer) months.

1139   Long term trends have been identified at locations in Mace Head, Ireland,

1140   midlatitudinal Canada, and Cape Point, South Africa, and varied over different

1141   time periods, which was speculated to be associated with changing anthropogenic

1142   and legacy emissions, and redox chemistry.

1143   2. For MBL GOM, diurnal variation was generally characterized with noon to

1144   afternoon peaks and nighttime low values and seasonal variation with higher

1145   concentrations in spring and summer and lower in fall and winter, largely

1146   attributed to GEM photooxidation as often supported by correlation of GOM with

1147   solar radiation and BrO. In one study springtime maximums were also linked to

1148   biological activity and in a few studies annual minimums were associated with

1149   scavenging by precipitation. No long term trends have been reported for oceanic

1150   regions.

1151   3. For MBL PBM, no consistent diurnal and seasonal variation has been identified in

1152   most studies, and only two studies reported seasonal variation with higher

1153   concentrations in fall/winter associated with anthropogenic emissions. One study

1154   showed no consistent diurnal variation in Tekran measurements but a clear diurnal

1155   cycle with maximums at noon and minimums before sunrise using 10-stage

1156   impactor measurements.

1157   4. For continental TGM/GEM, higher concentrations were found at urban sites than

1158   remote, rural, and elevated sites. This result is unbiased by elevated TGM/GEM

1159   from Asian sites. The predominant diurnal pattern was an early morning

1160   minimum and afternoon maximum, opposite to that at urban sites. Diurnal

1161   patterns at surface sites were thought to be driven by surface and local emissions,

1162   boundary layer dynamics, Hg photochemistry, dry deposition, and sequestering by

51

1163   dew. At elevated sites, mountain-valley winds appeared to be important drivers

1164   of the diurnal cycle. Seasonal variations were influenced by fossil fuel emissions

1165   for winter heating, surface emissions, and monsoons in Asia. At background sites,

1166   long-term declines in TGM were partially attributed to anthropogenic Hg

1167   emission reductions.

1168   5. For continental GOM, concentrations were higher at elevated sites. However, this

1169   result may be biased by a large proportion of high elevation studies from China

1170   where speciated atmospheric mercury are typically elevated. The predominant

1171   diurnal pattern was a noon to mid-afternoon maximum and nighttime minimum,

1172   except for nighttime increases at urban and elevated sites. The driving

1173   mechanisms of the diurnal variations were suggested to include in situ

1174   photochemical production, dry deposition, and scavenging by dew. Entrainment

1175   of GOM from the free troposphere was believed to contribute to nighttime

1176   increases at some elevated sites. No predominant seasonal pattern in GOM was

1177   found, except for higher concentrations in the spring/summer at urban sites.

1178   Photochemical production driven by strong solar radiation and atmospheric

1179   oxidants, free tropospheric transport, anthropogenic emissions, and increased wet

1180   deposition during summer appeared to affect GOM seasonal variation.

1181   6. For continental PBM or TPM, no predominant diurnal pattern was found.

1182   Increases in PBM or TPM were prevalent during colder seasons and were driven

1183   by local/regional coal combustion and wood burning emissions, lower mixing

1184   height, reduced oxidation, and increased gas-particle partitioning.

1185   7. TGM/GEM over the ocean surface decreased from the NH to the SH with the

1186   highest concentrations (~3.5 ng m^{-3}) in NH midlatitudes and the lowest in SH

1187   (~0.9 ng m^{-3}). This interhemispheric gradient was believed to suggest the

1188   majority of Hg emissions in NH, contradicting the hypothesis of large oceanic

1189   sources of Hg by previous work. However, in other studies the largest oceanic

1190   source was found in the equatorial region. Airborne measurements of TGM

1191   suggested distinct seasonal variation in latitudinal distributions, a ~50 ppqv (~0.5

1192   ng m^{-3}) increase in GEM concentrations from ~20°N – 30 °N to 60°N – 90°N

1193   latitudes in spring and negligible latitudinal variation in summer. It was

1194   speculated that smaller latitudinal gradient of temperature in summer likely

1195   enhanced meridional circulation resulting in smaller latitudinal variation in GEM

1196   concentration in the troposphere.

1197   8. GEM concentrations remained nearly constant, slightly decreasing with altitude

1198   over the several airborne field campaign regions, and depleted GEM was found in

1199   stratospherically influenced air masses. Abundant GOM has been suggested, but

1200   only very few studies have conducted measurements of free tropospheric GOM

1201   showing concentrations of hundreds of pg m^{-3}, particularly in the area of Pacific

1202   High.

1203   Over two decades of extensive measurements have advanced our knowledge of the

1204 spatiotemporal variation of TGM/GEM, GOM, and PBM in numerous continental and oceanic

1205 environments. However, measurement data, especially those of PBM, remain scarce in the SH,

1206 MBL, and upper air. In oceanic regions most observations, obtained via shipboard

1207 measurements of TGM/GEM with a few exceptions as ground-based on islands, suggested

1208 composite instead of instantaneous variation. Moreover, there are hardly size-fractionated PBM

1209   measurements. The current Tekran speciation unit could only measure PBM <2.5 μm, and

1210   Tekran PBM measurement data from a limited number of MBL and continental monitoring

1211   locations exhibited no definitive diurnal patterns in PBM concentrations. However, impactor

1212   measurements of total PBM in the MBL showed clearly-defined diurnal variation with daily

1213   maximums at around noon and minimums before sunrise. These existing problems impede our

1214   gaining full knowledge of global distributions and temporal variations of speciated Hg.

1215   GEM oxidation is one of the main driving mechanisms of diurnal and seasonal variations

1216   of TGM/GEM and GOM. However, the oxidants that are involved in the photochemical

1217   reactions driving the diurnal and seasonal variations of GOM remain largely unknown/uncertain,

1218   due to the lack of speciated GOM and upper air measurements. This is largely a result of

1219   inadequate technologies and a nebulous understanding of chemical reactions in atmospheric Hg

1220   transformation. Studies such as Chand et al. (2008) estimated GOM concentrations using the

1221   reaction of GEM + OH alone, and Sillman et al. (2007) reproduced observed GOM

1222   concentrations over Florida using CMAQ with gas-phase oxidation of GEM by O_3 and OH only.

1223   However, the reactions of GEM+ O_3 and GEM + OH have been subject to debate between

1224   theoretical and experimental studies, as no mechanism consistent with thermochemistry has been

1225   proposed (Pal and Ariya, 2004; Calvert and Lindberg, 2005; Subir et al., 2011; Ariya et al.,

1226   2015). It was speculated that GEM oxidation in the MBL and the upper troposphere was

1227   possibly largely Br-initiated (Holmes et al., 2009; Gratz et al., 2015; Shah et al., 2016). This

1228   indicated that even if a model reproduced observed concentrations of GOM, the chemistry in the

1229   model was not necessarily correct. So far, most chemical transport models have rarely focused

1230   on diurnal variation of speciated Hg; instead, they mostly focused on reproducing annual and

1231   monthly variations in TGM/GEM (Lei et al., 2013; Song et al., 2015), with large discrepancies

1232   between model simulations and surface measurements of GOM and PBM (Zhang et al., 2012;

1233   Kos et al., 2012). There are too many misrepresentations of Hg science and confounding issues

1234   in current models to gain a full understanding of the driving mechanisms for the observed diurnal

1235   to decadal variation in speciated Hg.

1236   In examining these unresolved questions and issues, the following recommendations for

1237   future research were hence suggested:

1238   • Global tropospheric distributions need to be mapped out for TGM/GEM, GOM, and

1239   PBM. Long-term monitoring of atmospheric Hg will need to be continued in time

1240   and space, particularly over oceans and at high altitudes utilizing innovative platforms,

1241   which undoubtedly demands technological breakthroughs in instrumentation.

1242   • Future research is warranted on GOM speciation measurements and multiphase redox

1243   kinetics. Field measurement studies need to include more oxidants besides ozone

1244   (and BrO in limited number of studies) in the analysis of diurnal variation.

1245   • Monitoring of long-term trends in TGM/GEM needs to continue, and more work is

1246   needed to unravel the causes responsible for the observed trends. Current hypotheses

1247   need to be validated using more extensive, longer datasets and a modeling system that

1248   includes realistic representation of dynamical, physical, and chemical processes in Hg

1249   cycling not only in the atmosphere but also in the ocean and between the two systems.

1250   • Size-fractionated PBM measurements are needed, including Hg concentrations on

1251   particles of all sizes, in space and time concurrent with TGM/GEM and GOM

1252   measurements.

1253   **Acknowledgements**

1255   of speciated atmospheric mercury data that are summarized and discussed in this review paper.

1256   Part of this work was funded by the Environmental Protection Agency grant agreement

1257   #83521501. We thank Ms. Y. Zhou for her help with Figure S1.

1258

1259   **Table Caption**

1260   Table 1: Summary of predominant temporal patterns of speciated atmospheric mercury at
1261   continental sites in the northern hemisphere
1262

1263   **Figure Captions**

1264   Figure 1. Means and ranges of TGM/GEM (a), GOM (b), and PBM (c) concentrations, estimated
1265   from the values in the literature as shown in Tables S1 – S3, over the Atlantic, Indian, Pacific,
1266   seas over the West Pacific (denoted as Pacific-Seas, only TGM/GEM in this category), seas in
1267   the Mediterranean region (denoted as Mediterranean), Arctic, and Antarctica Ocean. The solid
1268   black squares represent the mean value and the lowest whisker the minimum and the largest the
1269   maximum concentration in the region.
1270
1271   Figure 2. Median and range in TGM/GEM, GOM and PBM by site category (a) and by
1272   geographical region (b). Bar graph represents the median and error bar represents the maximum,
1273   estimated from the values in the literature as shown in Tables S4 – S6.
1274
1275   Figure 3. Compiled values for several marine/oceanic environmental systems. GEM over the
1276   Augusta basin is in red open circles. (Based on the figure from Bagnato et al., 2013)
1277
1278   Figure 4. GEM (ppqv) from the INTEX-B in spring 2006 and ARCTAS in spring and summer
1279   2008 (Data sources: Talbot et al., 2007, 2008; Mao et al., 2010).
1280

1281

References

1282   **References**

1283   Abbott, M. L., Lin, C. J., Martian, P., and Einerson, J. J.: Atmospheric mercury near Salmon
1284   Falls creek reservoir in southern Idaho, Appl. Geochem., 23(3), 438-453, 2008.

1285   Amos, H.M., Jacob, D. J., Kocman, D., Horowitz, H.M., Zhang, Y., Dutkiewicz, S., Horvat, M.,
1286   Corbitt, E.S., Krabbenhoft, D.P. and Sunderland, E.M.: Global biogeochemical implications of
1287   mercury discharges from rivers and sediment burial, M., et al.: Global biogeochemical
1288   implications of mercury discharges from rivers and sediment burial, Environ. Sci. Technol., 48
1289   (16), 9514-9522, 2014.

1290   Angot, H., M. Barret1, O. Magand, M. Ramonet, and A. Dommergue, A 2-year record of
1291   atmospheric mercury species at a background Southern Hemisphere station on Amsterdam Island,
1292   Atmos. Chem. Phys., 14, 11461–11473, 2014.

1293   Ariya, P. A., Amyot, M., Dastoor, A., Deeds, D., Feinberg, A., Kos, G., Poulain, A., Ryjkov, A.,
1294   Semeniuk, K., Subir, M., and Toyota, K.: Mercury physicochemical and biogeochemical
1295   transformation in the atmosphere and at atmospheric interfaces: a review and future directions,
1296   Chem. Rev., 115, 3760–3802, doi:10.1021/cr500667e, 2015.

1297   Aspmo, K., C. Temme, T. Berg, C. Ferrari, P.-A. Gauchard, X. Fain, and G. Wibetoe, Mercury
1298   in the atmosphere, snow, and melt water ponds in the North Atlantic Ocean during Arctic
1299   Summer, Environ. Sci. Technol., 40(13), 4083 – 4089, 2007.

1300   Bagnato, E., M. Sproverie, M. Barra, The sea–air exchange of mercury (Hg) in the marine
1301   boundary layer of the Augusta basin (southern Italy): Concentrations and evasion flux,
1302   Chemosphere, 93, 2024–2032, 2013.
1303
1304   Banic, C. M., S. T. Beauchamp, R. J. Tordon, W. H. Schroeder, A. Steffen, K. A. Anlauf, and H.
1305   K. T. Wong, Vertical distribution of gaseous elemental mercury in Canada, J. Geophys. Res.,
1306   108(D9), 4264, doi:10.1029/2002JD002116, 2003.
1307
1308   Beldowska, M., D. Saniewska, L. Falkowska, and A. Lewandowska, Mercury in particulate
1309   matter over Polish zone of the southern Baltic Sea, Atmos. Environ., 46, 397-404, 2012.
1310
1311   Berg, T., Pfaffhuber, K. A., Cole, A. S., Engelsen, O., and Steffen, A.: Ten-year trends in
1312   atmospheric mercury concentrations, meteorological effects and climate variables at Zeppelin,
1313   Ny-Ålesund, Atmos. Chem. Phys., 13(13), 6575-6586, 2013.
1314
1315   Brooks, S. X. Ren, M. Cohen, W. T. Luke, P. Kelley, R. Artz, A. Hynes, W. Landing, and B.
1316   Martos, Airborne Vertical Profiling of Mercury Speciation near Tullahoma, TN, USA, *Atmos.*, *5*,
1317   557-574; doi:10.3390/atmos5030557, 2014.
1318

1319　Brown, R. J., Goddard, S. L., Butterfield, D. M., Brown, A. S., Robins, C., Mustoe, C. L., and
1320　McGhee, E. A.: Ten years of mercury measurement at urban and industrial air quality monitoring
1321　stations in the UK, Atmos. Environ., 109, 1-8, 2015.
1322
1323　Brunke, E. G., Labuschagne, C., Ebinghaus, R., Kock, H.H., Slemr, F. Gaseous elemental
1324　mercury depletion events observed at Cape Point during 2007 and 2008, Atmos. Chem. Phys. 10,
1325　1121-1131, 2010.
1326
1327　Bullock, O. R. and Brehme, K. A.: Atmospheric mercury simulation using the CMAQ model:
1328　formulation description and analysis of wet deposition results, *Atmos. Environ.*, *36*(13), 2135-
1329　2146, 2002.
1330
1331　Calvert, J. G. and Lindberg, S. E.: Mechanisms of mercury removal by O3 and OH in the
1332　atmosphere, Atmos. Environ., *39*(18), 3355-3367, 2005.
1333
1334　Chand, D., et al. (2008), Reactive and particulate mercury in the Asian marine boundary layer,
1335　Atmos. Environ., 28, 7988–7996, doi:10.1016/j.atmosenv.2008.06.048.
1336
1337　Chen, L., Liu, M., Xu, Z., Fan, R., Tao, J., Chen, D., Zhang, D., Xie, D. and Sun, J.: Variation
1338　trends and influencing factors of total gaseous mercury in the Pearl River Delta—A highly
1339　industrialised region in South China influenced by seasonal monsoons, Atmos. Environ., 77,
1340　757-766, 2013.
1341
1342　Chen, L., Y. Zhang, D. J. Jacob, A. L. Soerensen, J. A. Fisher, H.M. Horowitz, E. S. Corbitt, and
1343　X. Wang (2015), A decline in Arctic Ocean mercury suggested by differences in decadal trends
1344　of atmospheric mercury between the Arctic and northern midlatitudes, Geophys. Res. Lett., 42,
1345　6076–6083, doi:10.1002/2015GL064051.
1346
1347　Cheng, I., Zhang, L., Blanchard, P., Dalziel, J., Tordon, R., Huang, J., and Holsen, T. M.:
1348　Comparisons of mercury sources and atmospheric mercury processes between a coastal and
1349　inland site, J. Geophys. Res. Atmos., 118(5), 2434-2443, 2013.
1350
1351　Cheng, I., Zhang, L., Blanchard, P., Graydon, J. A., and St. Louis, V. L.: Source-receptor
1352　relationships for speciated atmospheric mercury at the remote Experimental Lakes Area,
1353　northwestern Ontario, Canada, Atmos. Chem. Phys., 12(4), 1903-1922, 2012.
1354
1355　Cheng, I., Zhang, L., Mao, H., Blanchard, P., Tordon, R., and Dalziel, J.: Seasonal and diurnal
1356　patterns of speciated atmospheric mercury at a coastal-rural and a coastal-urban site, Atmos.
1357　Environ., 82, 193-205, 2014.
1358
1359　Choi, E. M., Kim, S. H., Holsen, T. M., and Yi, S. M.: Total gaseous concentrations in mercury
1360　in Seoul, Korea: local sources compared to long-range transport from China and Japan. Environ.
1361　Pollut., 157(3), 816-822, 2009.
1362
1363　Choi, H. D., Holsen, T. M., and Hopke, P. K.: Atmospheric mercury (Hg) in the Adirondacks:
1364　Concentrations and sources, Environ. Sci. Technol., 42(15), 5644-5653, 2008.

1365
1366 Choi, H. D., Huang, J., Mondal, S., and Holsen, T. M.: Variation in concentrations of three
1367 mercury (Hg) forms at a rural and a suburban site in New York State, Sci. Total Environ., 448,
1368 96-106, 2013.

1369 Ci, Z. J., Zhang, X. S., Wang, Z. W., Niu, Z. C., Diao, X. Y., Wang, S. W., Distribution and air-
1370 sea exchange of mercury (Hg) in the Yellow Sea, Atmos. Chem. Phys., 11, 2881–2892, doi:
1371 10.5194/acp-11-2881-2011, 2011.

1372 Civerolo, K. L., Rattigan, O. V., Felton, H. D., Hirsch, M. J., and DeSantis, S.: Mercury wet
1373 deposition and speciated air concentrations from two urban sites in New York State: Temporal
1374 patterns and regional context, Aerosol Air Qual. Res., 14(7), 1822-1837, 2014.
1375
1376 Cobbett, F. D., and Van Heyst, B. J.: Measurements of GEM fluxes and atmospheric mercury
1377 concentrations (GEM, RGM and Hgp) from an agricultural field amended with biosolids in
1378 Southern Ont., Canada (October 2004–November 2004), Atmos. Environ., 41(11), 2270-2282,
1379 2007.
1380
1381 Cole, A. S., A. Steffen, K. A. Pfaffhuber, T. Berg, M. Pilote, L. Poissant, R. Tordon, and H.
1382 Hung (2013), Ten-year trends of atmospheric mercury in the high Arctic compared to Canadian
1383 sub-Arctic and mid-latitude sites, Atmos. Chem. Phys., 13, 1535–1545, doi:10.5194/acp-13-
1384 1535-2013.
1385
1386 Cole, A. S., Steffen, A., Eckley, C. S., Narayan, J., Pilote, M., Tordon, R., Graydon, J. A., St.
1387 Louis, V.L., Xu, X., and Branfireun, B. A.: A survey of mercury in air and precipitation across
1388 Canada: patterns and trends, Atmosphere, 5(3), 635-668, 2014.

1389 Conaway, C. H., Mason, R. P., Steding, D. J., and Flegal, A. R.: Estimate of mercury emission
1390 from gasoline and diesel fuel consumption, San Francisco Bay area, California, Atmos. Environ.,
1391 39, 101–105, 2005.

1392 Dastoor, A. P., and D. A. Durnford, Arctic Ocean: is it a sink of a source of atmospheric mercury?
1393 Environ. Sci. Technol., 48, 1707−1717, 2014.

1394 De More, S. J., J. E. Patterson, D. M. Bibby, Baseline atmospheric mercury studies at Ross
1395 Island, Antarctica, Antarctic Sci., 5(3), 323-326, 1993.

1396 Dibble, T. S., Zelie, M. J., and Mao, H.: Thermodynamics of reactions of ClHg and BrHg
1397 radicals with atmospherically abundant free radicals, Atmos. Chem. Phys., *12*(21), 10271-10279,
1398 2012.
1399
1400 Driscoll, C. T., Mason, R. P., Chan, H. M., Jacob, D. J., and Pirrone, N.: Mercury as a global
1401 pollutant: sources, pathways, and effect, Environ. Sci. Technol., *47*(10), 4967-4983, 2013.
1402
1403 Ebinghaus, R., and F. Slemr, Aircraft measurements of atmospheric mercury over southern and
1404 eastern Germany, Atmos. Environ., 34, 895-903, 2000.

1405
1406 Ebinghaus, R., F. Slemr, C.A.M. Brenninkmeijer, P. van Velthoven, A. Zahn,M.Hermann, D. A.
1407 O'Sullivan, and D. E. Oram (2007), Emissions of gaseous mercury from biomass burning in
1408 South America in 2005 observed during CARIBIC flights, Geophys. Res. Lett., 34, L08813,
1409 doi:10.1029/2006GL028866.
1410
1411 Ebinghaus, R., Jennings, S. G., Kock, H. H., Derwent, R. G., Manning, A. J., and Spain, T. G.:
1412 Decreasing trends in total gaseous mercury observations in baseline air at Mace Head, Ireland
1413 from 1996 to 2009, Atmos. Environ., 45(20), 3475-3480, 2011.
1414
1415 Ebinghaus, R., Kock, H. H., Coggin, AM, Spain, TG, Jennings, SG, Temme, C., Long term
1416 measurements of atmospheric mercury at Mace Head, Irish west coast, between 1995 and 2001.
1417 Atmos. Environ., 36, 5267 – 76, 2002a.
1418
1419 Ebinghaus, R., Kock, H. H., Temme, C., Einax, J. W., Löwe, A. G., Richter, A., Burrows, J. P.,
1420 Schroeder, W. H., Antarctic springtime depletion of atmospheric mercury, Environ. Sci.
1421 Technol., 36, 1238-1244, 2002b.
1422
1423 Eckley, C.S., Parsons, M.T., Mintz, R., Lapalme, M., Mazur, M., Tordon, R., Elleman, R.,
1424 Graydon, J.A., Blanchard, P. and St. Louis, V.: Impact of closing Canada's largest point-source
1425 of mercury emissions on local atmospheric mercury concentrations, Environ. Sci. Technol.,
1426 47(18), 10339-10348, 2013.
1427
1428 Engle, M. A., Tate, M. T., Krabbenhoft, D. P., Schauer, J. J., Kolker, A., Shanley, J. B., and
1429 Bothner, M. H.: Comparison of atmospheric mercury speciation and deposition at nine sites
1430 across central and eastern North America, J. Geophys. Res. Atmos., 115(D18), 2010.
1431
1432 Faïn, X., Obrist, D., Hallar, A. G., Mccubbin, I., and Rahn, T.: High levels of reactive gaseous
1433 mercury observed at a high elevation research laboratory in the Rocky Mountains, Atmos. Chem.
1434 Phys., 9(20), 8049-8060, 2009.
1435
1436 Feddersen, D. M., Talbot, R., Mao, H., and Sive, B. C.: Size distribution of particulate mercury
1437 in marine and coastal atmospheres, Atmos. Chem. Phys., *12*(22), 10899-10909, 2012.
1438
1439 Fisher, J. A., D. J. Jacob, A. L. Soerensen, H. M. Amos, E. S. Corbitt, D. G. Streets, Q. Wang, R.
1440 M. Yantosca, and E. M. Sunderland (2013), Factors driving mercury variability in the Arctic
1441 atmosphere and ocean over the past 30 years, Global Biogeochem. Cycles, 27, 1226–1235,
1442 doi:10.1002/2013GB004689.
1443
1444 Fisher, J. A., Jacob, D. J., Soerensen, A. L., Amos, H. M., Steffen, A. & Sunderland, E. M.:
1445 Riverine source of Arctic Ocean mercury inferred from atmospheric observations. Nature
1446 Geoscience, 5(7), 499-504, 2012
1447
1448 Fitzgerald, W.F.: Is mercury increasing in the atmosphere? The need for an atmospheric mercury
1449 network (AMNET). Water, Air and Soil Pollut., 80, 245-254, 1995.
1450

1451   Fitzgerald, W.F., Gill, G.A., Kim, J.P., 1984. An Equatorial Paci"c source of atmospheric ercury.
1452   Science, 224, 597-599.
1453
1454   Fitzgerald, W.F., Mason, R.P., 1996. The global mercury cycle: oceanic and anthropogenic
1455   aspects. In: Baeyens, W., Ebinghaus, R., Vasiliev, O. (Eds.), Global and Regional Mercury
1456   Cycles: Sources, Fluxes and Mass Balances. NATO ASI Series 2. Environment, vol. 21. Kluwer
1457   Ac. Pub., Dordrecht, pp. 85-108.
1458
1459   Fostier, A. H. and Michelazzo, P. A.: Gaseous and particulate atmospheric mercury
1460   concentrations in the Campinas Metropolitan Region (Sao Paulo State, Brazil), J. Brazilian
1461   Chem. Soc., 17(5), 886-894, 2006.
1462
1463   Friedli, H. R., L. F. Radke, R. Prescott, P. Li, J.-H. Woo, and G. R. Carmichael (2004), Mercury
1464   in the atmosphere around Japan, Korea, and China as observed during the 2001 ACE-Asia field
1465   campaign: Measurements, distributions, sources, and implications, J. Geophys. Res., 28, D19S25,
1466   doi:10.1029/2003JD004244.
1467
1468   Fu, X. W., Feng, X., Dong, Z. Q., Yin, R. S., Wang, J. X., Yang, Z. R., and Zhang, H.:
1469   Atmospheric gaseous elemental mercury (GEM) concentrations and mercury depositions at a
1470   high-altitude mountain peak in south China, Atmos. Chem. Phys., 10(5), 2425-2437, 2010.
1471
1472   Fu, X. W., Feng, X., Liang, P., Zhang, H., Ji, J., and Liu, P.:Temporal trend and sources of
1473   speciated atmospheric mercury at Waliguan GAW station, Northwestern China, Atmos. Chem.
1474   Phys., 12(4), 1951-1964, 2012a.
1475
1476   Fu, X. W., Feng, X., Shang, L. H., Wang, S. F., and Zhang, H.: Two years of measurements of
1477   atmospheric total gaseous mercury (TGM) at a remote site in Mt. Changbai area, Northeastern
1478   China, Atmos. Chem. Phys., 12, 4215-4226, doi:10.5194/acp-12-4215-2012, 2012b.
1479
1480   Fu, X. W., Zhang, H., Yu, B., Wang, X., Lin, C.-J., and Feng, X. B.: Observations of
1481   atmospheric mercury in China: a critical review, Atmos. Chem. Phys., 15, 9455-9476,
1482   doi:10.5194/acp-15-9455-2015, 2015.
1483
1484   Fu, X., Feng, X., Wang, S., Rothenberg, S., Shang, L., Li, Z., and Qiu, G.: Temporal and spatial
1485   distributions of total gaseous mercury concentrations in ambient air in a mountainous area in
1486   southwestern China: Implications for industrial and domestic mercury emissions in remote areas
1487   in China, Sci. Total Environ., 407(7), 2306-2314, 2009.
1488
1489   Fu, X., Feng, X., Zhang, G., Xu, W., Li, X., Yao, H., Liang, P., Li, J., Sommar, J., Yin, R., and
1490   Liu, N.: Mercury in the marine boundary layer and seawater of the South China Sea:
1491   Concentrations, sea/air flux, and implication for land outflow, J. Geophys. Res., 115, D06303,
1492   doi:10.1029/2009JD012958, 2010.
1493
1494   Fu, X., Feng, X., Zhu, W., Wang, S., and Lu, J.: Total gaseous mercury concentrations in
1495   ambient air in the eastern slope of Mt. Gongga, South-Eastern fringe of the Tibetan plateau,
1496   China, Atmos. Environ., 42(5), 970-979, 2008.

1497
1498 Gay, D. A., Schmeltz, D., Prestbo, E., Olson, M., Sharac, T., and Tordon, R.: The Atmospheric
1499 Mercury Network: measurement and initial examination of an ongoing atmospheric mercury
1500 record across North America, Atmos. Chem. Phys., 13(22), 11339-11349, 2013.
1501 Geoscience, 5(7), 499-504.
1502
1503 Gratz, L. E., Ambrose, J.L., Jaffe, D.A., Shah, V., Jaeglé, L., Stutz, J., Festa, J., Spolaor, M., Tsai,
1504 C., Selin, N.E. and Song, S: Oxidation of mercury by bromine in the subtropical Pacific free
1505 troposphere, Geophys. Res. Lett., 42, 10,494–10,502, doi:10.1002/2015GL066645, 2015.
1506
1507 Gratz, L. E., Keeler, G. J., Marsik, F. J., Barres, J. A., and Dvonch, J. T.: Atmospheric transport
1508 of speciated mercury across southern Lake Michigan: Influence from emission sources in the
1509 Chicago/Gary urban area, Sci. Total Environ., 448, 84-95, 2013.
1510
1511 Hall, C.B., Mao, H., Ye, Z., Talbot, R., Ding, A., Zhang, Y., Zhu, J., Wang, T., Lin, C.J., Fu, C.
1512 and Yang, X.: Sources and Dynamic Processes Controlling Background and Peak Concentrations
1513 of TGM in Nanjing, China, Atmosphere, 5(1), 124-155, 2014.
1514
1515 Han, Y. J., Kim, J. E., Kim, P. R., Kim, W. J., Yi, S. M., Seo, Y. S., and Kim, S. H.: General
1516 trends of atmospheric mercury concentrations in urban and rural areas in Korea and
1517 characteristics of high-concentration events, Atmos. Environ., 94, 754-764, 2014.
1518
1519 Hedgecock I. M., and N. Pirrone, Chasing quicksilver: modeling the atmospheric lifetime of Hg0
1520 (g) in the marine boundary layer at various latitudes. Environ. Sci. Technol., 38, 69–76, 2004.
1521
1522 Hedgecock, I. M., G. A. Trunfio, N. Pirrone, and F. Sprovieri (2005), Mercury chemistry in the
1523 MBL: Mediterranean case and sensitivity studies using the AMCOTS (Atmospheric Mercury
1524 Chemistry over the Sea) model, Atmos. Environ., 39, 7217– 7230.
1525
1526 Hedgecock, I. M., N. Pirrone, F. Sprovieri, and E. Pesenti (2003), Reactive gaseous mercury in
1527 the marine boundary layer: Modelling and experimental evidence of its formation in the
1528 Mediterranean region, Atmos. Environ., 37, suppl. 1, S41– S49.
1529
1530 Huang, J., Choi, H. D., Hopke, P. K., and Holsen, T. M.: Ambient mercury sources in Rochester,
1531 NY: results from principle components analysis (PCA) of mercury monitoring network data,
1532 Environ. Sci. Technol., 44(22), 8441-8445, 2010.
1533
1534 Holmes, C. D., Jacob, D. J., and Yang, X.: Global lifetime of elemental mercury against
1535 oxidation by atomic bromine in the free troposphere, Geophys. Res. Lett., 33, L20808,
1536 doi:10.1029/2006GL027176, 2006.
1537
1538 Holmes, C. D., Jacob, D. J., Mason, R. P., and Jaffe, D. A.: Sources and deposition of reactive
1539 gaseous mercury in the marine atmosphere, Atmos. Environ., 43(14), 2278-2285, 2009.
1540
1541 Hynes, A. J., Donohoue, D. L., Goodsite, M. E., and Hedgecock, I. M.: Our current
1542 understanding of major chemical and physical processes affecting mercury dynamics in the

1543 atmosphere and at the air-water/terrestrial interfaces, Pirrone, N. and Mason, R. (Eds.), In
1544 Mercury fate and transport in the global atmosphere (pp. 427-457). Springer U.S., 2009.

1545

1546 Jiang, Y., Cizdziel, J. V., and Lu, D.: Temporal patterns of atmospheric mercury species in
1547 northern Mississippi during 2011–2012: Influence of sudden population swings, Chemosphere,
1548 93(9), 1694-1700, 2013.

1549 Kang, H, and Z. Xie, Atmospheric mercury over the marine boundary layer observed during the
1550 third China Arctic Research Expedition, J. Environ. Sci., 23(9), 1424–1430, 2011.

1551 Kim, J. and Fitzgerald, W.: Gaseous mercury profiles in the tropical Pacific Ocean, Geophys.
1552 Res. Lett., *15*(1), 40-43, 1988.

1553 Kim, K. H., Yoon, H. O., Brown, R. J., Jeon, E. C., Sohn, J. R., Jung, K., Park, C. G., and Kim, I.
1554 S.: Simultaneous monitoring of total gaseous mercury at four urban monitoring stations in Seoul,
1555 Korea, Atmos. Res., 132, 199-208, 2013.

1556

1557 Kim, P. R., Han, Y. J., Holsen, T. M., and Yi, S. M.: Atmospheric particulate mercury:
1558 Concentrations and size distributions, Atmos. Environ., 61, 94-102, 2012.

1559

1560 Kolker, A., Olson, M. L., Krabbenhoft, D. P., Tate, M. T., and Engle, M. A.: Patterns of mercury
1561 dispersion from local and regional emission sources, rural Central Wisconsin, USA, Atmos.
1562 Chem. Phys., 10(10), 4467-4476, 2010.

1563

1564 Kos G., Ryzhkov A., Dastoor A., Narayan J., Steffen A., Ariya P.A., and Zhang L., 2013.
1565 Evaluation of discrepancy between measured and modelled oxidized mercury species.
1566 Atmospheric Chemistry and Physics, 13, 4839-4863.

1567

1568 Kotnik, J., Sprovieri, F., Ogrinc, N., Horvat, M., and Pirrone, N.: Mercury in the Mediterranean,
1569 part I: spatial and temporal trends, *Environ. Sci. Pollut. Res.*, *21*(6), 4063-4080, 2014.

1570

1571 Lamborg, C. H., K. R. Rolfhus, and W. F. Fitzgerald, The atmospheric cycling and air-sea
1572 exchange of mercury species in the south and equatorial Atlantic Ocean, Deep Sea Res., Part II,
1573 46, 957– 977, 1999.

1574

1575 Lan, X., Talbot, R., Castro, M., Perry, K., and Luke, W.: Seasonal and diurnal variations of
1576 atmospheric mercury across the US determined from AMNet monitoring data, Atmos. Chem.
1577 Phys., 12(21), 10569-10582, 2012.

1578

1579 Lan, X., Talbot, R., Laine, P., Lefer, B., Flynn, J., and Torres, A.: Seasonal and diurnal
1580 variations of total gaseous mercury in urban Houston, TX, USA, Atmosphere, 5(2), 399-419,
1581 2014.

1582

1583 Landis, M. S., Lewis, C. W., Stevens, R. K., Keeler, G. J., Dvonch, J. T., and Tremblay, R. T.: Ft.
1584 McHenry tunnel study: Source profiles and mercury emissions from diesel and gasoline powered
1585 vehicles, Atmos. Environ., 41, 8711–8724, 2007.

Laurier, F. J. G., R. P. Mason, L. Whalin, and S. Kato, Reactive gaseous mercury formation in the North Pacific Ocean's marine boundary layer: A potential role of halogen chemistry, J. Geophys. Res., 108(D17), 4529, doi:10.1029/2003JD003625, 2003.

Laurier, F., and R. Mason, Mercury concentration and speciation in the coastal and open ocean boundary layer, J. Geophys. Res., 112, D06302, doi:10.1029/2006JD007320.

Lei, H., Liang, X.-Z., Wuebbles, D. J., and Tao, Z.: Model analyses of atmospheric mercury: present air quality and effects of transpacific transport on the United States, Atmos. Chem. Phys., 13, 10807-10825, doi:10.5194/acp-13-10807-2013, 2013.

Li, J., Sommar, J., Wängberg, I., Lindqvist, O., and Wei, S. Q.: Short-time variation of mercury speciation in the urban of Göteborg during GÖTE-2005, Atmos. Environ., 42(36), 8382-8388, 2008.

Li, Z., Xia, C., Wang, X., Xiang, Y., and Xie, Z.: Total gaseous mercury in Pearl River Delta region, China during 2008 winter period, Atmos. Environ., 45(4), 834-838, 2011.

Lindberg, Lindberg, S. E. et al. Dynamic oxidation of gaseous mercury in the Arctic troposphere at polar sunrise. Environ. Sci. Tech. 36, 1245-1256, 2002.

Liu, B., Keeler, G. J., Dvonch, J. T., Barres, J. A., Lynam, M. M., Marsik, F. J., and Morgan, J. T.: Temporal variability of mercury speciation in urban air. Atmos. Environ., 41(9), 1911-1923, 2007.

Liu, B., Keeler, G. J., Dvonch, J. T., Barres, J. A., Lynam, M. M., Marsik, F. J., and Morgan, J. T.: Urban–rural differences in atmospheric mercury speciation, Atmos. Environ., 44(16), 2013-2023, 2010.

Lyman, S. N. and Gustin, M. S.: Speciation of atmospheric mercury at two sites in northern Nevada, USA, Atmos. Environ., 42(5), 927-939, 2008.

Lyman, S. N., and D. A. Jaffe, Formation and fate of oxidized mercury in the upper troposphere and lower stratosphere, Nature Geosci., DOI: 10.1038/NGEO1353, 2011.

Lyman, S. N., and Gustin, M. S.: Determinants of atmospheric mercury concentrations in Reno, Nevada, USA, Sci. Total Environ., 408(2), 431-438, 2009.

Lynam, M. M. and Keeler: Automated speciated mercury measurements in Michigan, Environ. Sci. Technol., 39(23), 9253-9262, 2005.

Malcolm, E. G.; Keeler, G. J.; Landis, M. S. The effects of the coastal environment on the atmospheric mercury cycle. *J. Geophys. Res.* 2003, *108*, article no. 4357.

Manolopoulos, H., Schauer, J. J., Purcell, M. D., Rudolph, T. M., Olson, M. L., Rodger, B., and Krabbenhoft, D. P.: Local and regional factors affecting atmospheric mercury speciation at a remote location. J. Environ. Eng. Sci., 6(5), 491-501, 2007.

Mao, H., Talbot, R. W., Sigler, J. M., Sive, B. C., and Hegarty, J. D.: Seasonal and diurnal variations of Hg over New England, Atmos. Chem. Phys., 8(5), 1403-1421, 2008.

Mao, H. and Talbot, R.: Speciated mercury at marine, coastal, and inland sites in New England–Part 1: Temporal variability, Atmos. Chem. Phys., 12(11), 5099-5112, 2012.

Mao, H., Talbot, R., Hegarty, J., and Koermer, J.: Speciated mercury at marine, coastal, and inland sites in New England–Part 2: Relationships with atmospheric physical parameters, Atmos. Chem. Phys., 12(9), 4181-4206, 2012.

Mao, H., Talbot, R. W., Sive, B. C., Kim, S. Y., Blake, D. R., and Weinheimer, A. J.: Arctic mercury depletion and its quantitative link with halogens, *J. Atmos. Chem.*, *65*(2-3), 145-170, 2010.

Marumoto, K., Hayashi, M., and Takami, A.: Atmospheric mercury concentrations at two sites in the Kyushu Islands, Japan, and evidence of long-range transport from East Asia, Atmos. Environ., 117, 147-155, 2015.

Mason, R. P., and G.-R. Sheu, Role of the ocean in the global mercury cycle, Global Biogeochem. Cycles, 16(4), 1093, 10.1029/2001GB001440, 2002.

Mason, R. P.; Lawson, N. M.; Sheu, G.-R. Mercury in the Atlantic Ocean: factors controlling air-sea exchange of mercury and its distribution in the upper waters. *Deep-Sea Res. II.*, *48*, 2829-2853, 2001.

Mason, R.P., Fitzgerald, W.F., Morel, F.M., 1994. The biogeochemical cycling of elemental mercury: anthropogenic influences, Geochimica et Cosmochimica Acta, 58, 3191–3198.

Mason, R.P., Fitzgerald, W.F., Vandal, G.M., 1992. The sources of mercury in Equatorial Pacific rain. Journal of Atmospheric Chemistry 14, 489-500.

Mazur, M., Mintz, R., Lapalme, M., and Wiens, B.: Ambient air total gaseous mercury concentrations in the vicinity of coal-fired power plants in Alberta, Canada, Sci. Total Environ., 408(2), 373-381, 2009.

Moore, C., D. Obrist, M. Luria, Atmospheric mercury depletion events at the Dead Sea: Spatial and temporal aspects, Atmos. Environ., 69, 231-239, 2013.

Müller, D., Wip, D., Warneke, T., Holmes, C. D., Dastoor, A., and Notholt, J.: Sources of atmospheric mercury in the tropics: continuous observations at a coastal site in Suriname, Atmos. Chem. Phys., 12, 7391–7397, doi:10.5194/acp-12-7391-2012, 2012.

Murphy, D. M., Thomson, D. S., and Mahoney, M. J.: In situ measurements of organics, meteoritic material, mercury, and other elements in aerosols at 5 to 19 kilometers, *Science*, *282*(5394), 1664-1669, 1998.

Murphy, D. M., Hudson, P. K., Thomson, D. S., Sheridan, P. J., and Wilson, J. C.: Observations of mercury-containing aerosols, Environ. Sci. Technol., *40*(10), 3163-3167, 2006.

 Nair, U. S., Wu, Y., Walters, J., Jansen, J., and Edgerton, E. S.: Diurnal and seasonal variation of mercury species at coastal-suburban, urban, and rural sites in the southeastern United States, Atmos. Environ., 47, 499-508, 2012.

Nguyen, D. L., Kim, J. Y., Shim, S. G., and Zhang, X. S.: Ground and shipboard measurements of atmospheric gaseous elemental mercury over the Yellow Sea region during 2007–2008. Atmos. Environ., 45(1), 253-260, 2011.

Obrist, D., E. Tas, M. Peleg, V. Matveev, X. Faïn, D. Asaf, and M. Lur, Bromine-induced oxidation of mercury in the mid-latitude atmosphere, Nature Geosci., 4, 22 – 26, 2011.

Obrist, D., Hallar, A. G., McCubbin, I., Stephens, B. B., and Rahn, T.: Atmospheric mercury concentrations at Storm Peak Laboratory in the Rocky Mountains: Evidence for long-range transport from Asia, boundary layer contributions, and plant mercury uptake, Atmos. Environ., 42(33), 7579-7589, 2008.

Pal, B. and Ariya, P. A.: Gas-phase HO-initiated reactions of elemental mercury: kinetics, product studies, and atmospheric implications, Environ. Sci. Technol., 38, 5555–5566, 2004.

Parsons, M. T., McLennan, D., Lapalme, M., Mooney, C., Watt, C., and Mintz, R.: Total gaseous mercury concentration measurements at Fort McMurray, Alberta, Canada, Atmosphere, 4(4), 472-493, 2013.

Peterson, C., Gustin, M., and Lyman, S.: Atmospheric mercury concentrations and speciation measured from 2004 to 2007 in Reno, Nevada, USA, Atmos. Environ., 43(30), 4646-4654, 2009.

Pfaffhuber, K. A., Berg, T., Hirdman, D., and Stohl, A.: Atmospheric mercury observations from Antarctica: seasonal variation and source and sink region calculations, Atmos. Chem. Phys., 12, 3241–3251, doi:10.5194/acp-12-3241-2012, 2012.

Pirrone, N., Ferrara, R., Hedgecock, I.M., Kallos, G., Mamane, Y., Munthe, J., Pacyna, J.M., Pytharoulis, I., Sprovieri, F., Voudouri, A. and Wangberg, I.: Dynamic processes of atmospheric mercury over the Mediterranean region, Atmos. Environ. , 37(S1), 21–40, 2003.

Pirrone, N., Cinnirella,S., Feng, X., Finkelman,R. B.,Friedli, H. R., Leaner, J., Mason, R., Mukherjee, A. B., Stracher, G. B., Streets, D. G., and Telmer, K.: Global mercury emissions to the atmosphere from anthropogenic and natural sources, Atmos. Chem. Phys., 10, 59515951-5964, 2010.

1722 Pongratz, R., and K. Heumann, Production of methylated mercury, lead, and cadmium by marine
1723 bacteria as a significant natural source for atmospheric heavy metals in polar regions,
1724 Chemosphere, 39, 89– 102, 1999.

1726 Prestbo, E.M. 1997. Mercury speciation in the boundary layer and free troposphere advected to
1727 South Florida: Phase I - Reconnaissance. Report to the Florida Department of Environmental
1728 Protection, Tallahassee. Frontier Geosciences, Seattle, WA.

1730 Radke, L. F., H. R. Friedli, and B. G. Heikes (2007), Atmospheric mercury over the NE Pacific
1731 during spring 2002: Gradients, residence time, upper troposphere lower stratosphere loss, and
1732 long-range transport, J. Geophys. Res., 112, D19305, doi:10.1029/2005JD005828.

1734 Rothenberg, S. E., McKee, L., Gilbreath, A., Yee, D., Connor, M., and Fu, X.: Evidence for
1735 short-range transport of atmospheric mercury to a rural, inland site, Atmos. Environ., 44(10),
1736 1263-1273, 2010.

1738 Rutter, A. P., and Schauer, J. J.: The effect of temperature on the gas–particle partitioning of
1739 reactive mercury in atmospheric aerosols, Atmos. Environ., 41(38), 8647-8657, 2007.

1741 Rutter, A. P., Schauer, J. J., Lough, G. C., Snyder, D. C., Kolb, C. J., Von Klooster, S., Rudolf,
1742 T., Manolopoulos, H., and Olson, M. L.: A comparison of speciated atmospheric mercury at an
1743 urban center and an upwind rural location. J. Environ. Monit., 10(1), 102-108, 2008.

1745 Rutter, A.P., Snyder, D. C., Stone, E.A., Schauer, J.J., Gonzalez-Abraham, R., Molina, L.T.,
1746 Márquez, C., Cárdenas, B. and Foy, B.D.: In situ measurements of speciated atmospheric
1747 mercury and the identification of source regions in the Mexico City Metropolitan Area, Atmos.
1748 Chem. Phys., 9(1), 207-220, 2009.

1750 Sander, R.; Keene, W. C.; Pszenny, A. A. P.; Arimoto, R.; Ayers, G. P.; Baboukas, E.; Cainey, J.
1751 M.; Crutzen, P. J.; Duce, R. A.; Honninger, G.; Huebert, B. J.; Maenhaut, W.; Mihalopoulos, N.;
1752 Schleicher, N. J., Schäfer, J., Blanc, G., Chen, Y., Chai, F., Cen, K., and Norra, S.: Atmospheric
1753 particulate mercury in the megacity Beijing: Spatio-temporal variations and source
1754 apportionment, Atmos. Environ., 109, 251-261, 2015.

1756 Schroeder, W. H., Anlauf, K. G., Barrie, L. A., Lu, J. Y., Steffen, A., Schneeberger, D. R., and
1757 Berg, T. : Arctic springtime depletion of mercury, Nature, 394, 331-332, 1998.

1759 Schroeder, W. H., and Munthe, J.: Atmospheric mercury—an overview, Atmos. Environ., *32*(5),
1760 809-822, 1998.

1761 Seiler, W., C. Eberling, and G. Slemr, Global distribution of gaseous mercury in the troposphere,
1762 Pageoph, 118, 964 – 974, 1980.

1763 Selin, N. E., D. J. Jacob, R. J. Park, R. M. Yantosca, S. A. Strode, L. Jaegle, and D. Jaffe (2007),
1764 Chemical cycling and deposition of atmospheric mercury: Global constraints from observations,
1765 J. Geophys. Res., 112, D02308, doi:10.1029/2006JD007450.

1766
1767   Shah, V., et al., Origin of oxidized mercury in the summertime free troposphere over the
1768   southeastern US, Atmos. Chem. Phys., 16, 1511–1530, 2016.
1769
1770   Sheu, G. R., Lin, N. H., Wang, J. L., Lee, C. T., Yang, C. F. O., and Wang, S. H.: Temporal
1771   distribution and potential sources of atmospheric mercury measured at a high-elevation
1772   background station in Taiwan, Atmos. Environ., 44(20), 2393-2400, 2010.
1773
1774   Sheu, G.-R., and R. P. Mason (2001), An examination of methods for the measurements of
1775   reactive gaseous mercury in the atmosphere, Environ. Sci. Technol., 35, 1209–1216.
1776
1777   Sheu, G.-R., and R. P. Mason (2004), An examination of the oxidation of elemental mercury in
1778   the presence of halide surfaces, J. Atmos. Chem., 48, 107–130.
1779
1780   Sheu, G.-R., Speciation and distribution of atmospheric mercury: Significance of reactive
1781   gaseous mercury in the global mercury cycle, Ph.D. thesis, 170 pp., Univ. of Md., College Park,
1782   2001.
1783
1784   Sigler, J. M., Mao, H., and Talbot, R.: Gaseous elemental and reactive mercury in Southern New
1785   Hampshire, Atmos. Chem. Phys., 9(6), 1929-1942, 2009a.
1786
1787   Sigler, J. M., Mao, H., Sive, B., and Talbot, R., Oceanic Influence on Atmospheric Mercury at
1788   Coastal and Inland Sites: A Springtime Nor'easter in New England, *Atmos. Chem. Phys.,*
1789   *9*, 4023-4030, 2009b.
1790
1791   Sillman, S., Marsik, F. J., Al-Wali, K. I., Keeler, G. J., and Landis, M. S.: Reactive mercury in
1792   the troposphere: Model formation and results for Florida, the northeastern United States, and the
1793   Atlantic Ocean, *J. Geophys. Res. Atmos.*, *112*(D23305), doi:10.1029/2006JD008227, 2007.
1794
1795   Siudek, P., Frankowski, M., and Siepak, J.: Atmospheric particulate mercury at the urban and
1796   forest sites in central Poland, Environ. Sci. Pollut. Res., 23(3), 2341-2352, 2016.
1797
1798   Slemr, F., Angot, H., Dommergue, A., Magand, O., Barret, M., Weigelt, A., Ebinghaus, R.,
1799   Brunke, E.-G., Pfaffhuber, K. A., Edwards, G., Howard, D., Powell, J., Keywood, M., and Wang,
1800   F.: Comparison of mercury concentrations measured at several sites in Southern Hemisphere,
1801   submitted to Atmos. Chem. Phys., 15, 3125–3133, 2015.
1802
1803   Slemr, F., Brunke, E.-G., Ebinghaus, R., Kuss, J., Worldwide trend of atmospheric mercury since
1804   1995. Atmos. Chem. Phys., 11, 4779-4787, 2011.
1805
1806   Slemr, F., E.-G. Brunke, C. Labuschagne, and R. Ebinghaus (2008), Total gaseous mercury
1807   concentrations at the Cape Point GAW station and their seasonality, Geophys. Res. Lett., 35,
1808   L11807, doi:10.1029/2008GL033741.
1809
1809   Slemr, F., G. Schuster, W. Seiler, Distribution, speciation, and budget of atmospheric mercury, J.
1810   Atmos. Chem., 3(4), 407-434, 1985.

1811 Slemr, F., Trends in atmospheric mercury concentrations over the Atlantic ocean and the Wank
1812 summit, and the resulting constraints on the budget of atmospheric mercury, in "*Global and*
1813 *Regional Mercury Cycles: Sources, Fluxes and Mass Balances*", eds. W. Bayyens, R. Ebinghaus,
1814 and O. Vasiliev, NATO-ASI-Series, Vol. 21, pp 33-84, Kluwer Academic Publishers, Dordrecht,
1815 The Netherlands, 1996.

1816 Slemr, F., W. JunkermannR, .W. H. Schmidt, and R. Sladkovic, Indication of change in global
1817 and regional trends of atmospheric mercury concentrations, Geophys. Res. Lett., 22(16), 2143-
1818 2146, 1995.
1819
1820 Slemr, F. and Langer, E.: Increase in global atmospheric concentrations of mercury inferred from
1821 measurements over the Atlantic Ocean, *Nature* **355**, 434 – 437, 1992.

1822 Slemr, F., W. Seiler, and G. Schuster, Latitudinal distribution of mercury over the Atlantic
1823 Ocean, J. Geophys. Res., 86, C2, 1159-1166, 1981.

1824 Soerensen, A. L., D. J. Jacob, D. G. Streets, M. L. I. Witt, R. Ebinghaus, R. P. Mason, M.
1825 Andersson, and E.M. Sunderland (2012), Multi-decadal decline of mercury in the North Atlantic
1826 atmosphere explained by changing subsurface seawater concentrations, Geophys. Res. Lett., 39,
1827 L21810, doi:10.1029/2012GL053736.
1828
1829 Soerensen, A. L., H. Skov, D. J. Jacob, B. T. Soerensen, M. S. Johnson, Global Concentrations
1830 of Gaseous Elemental Mercury and Reactive Gaseous Mercury in the Marine Boundary Layer,
1831 Environ Sci Technol., 44(19), 7425-30. doi: 10.1021/es903839n, 2010.
1832
1833 Sommar, J., M. E. Anersson, and H.-W. Jacobi, Circumpolar measurements of speciated mercury,
1834 ozone and carbon monoxide in the boundary layer of the Arctic Ocean, Atmos. Chem. Phys., 10,
1835 5031–5045, 2010.
1836
1837 Song, S., Selin, N. E., Soerensen, A. L., Angot, H., Artz, R., Brooks, S., Brunke, E.-G., Conley,
1838 G., Dommergue, A., Ebinghaus, R., Holsen, T. M., Jaffe, D. A., Kang, S., Kelley, P., Luke, W.
1839 T., Magand, O., Marumoto, K., Pfaffhuber, K. A., Ren, X., Sheu, G.-R., Slemr, F., Warneke, T.,
1840 Weigelt, A., Weiss-Penzias, P., Wip, D. C., and Zhang, Q.: Top-down constraints on
1841 atmospheric mercury emissions and implications for global biogeochemical cycling, Atmos.
1842 Chem. Phys., 15, 7103-7125, doi:10.5194/acp-15-7103-2015, 2015.
1843
1844 Song, X., Cheng, I., and Lu, J.: Annual atmospheric mercury species in downtown Toronto,
1845 Canada, J. Environ. Monit., 11(3), 660-669, 2009.
1846
1847 Sprovieri, F. and Pirrone, N., Spatial and temporal distribution of atmospheric mercury species
1848 over the Adriatic Sea, Environ. Fluid Mech., 8, 117–128, doi:10.1007/s10652-007-9045-4, 2008.
1849
1850 Sprovieri, F., I. M. Hedgecock, and N. Pirrone, An investigation of the origins of reactive
1851 gaseous mercury in the Mediterranean marine boundary layer, Atmos. Chem. Phys., 10, 3985–
1852 3997, 2010a.
1853

1854 Sprovieri, F., N. Pirrone, I. M. Hedgecock, M. S. Landis, and R. K. Stevens, Intensive
1855 atmospheric mercury measurements at Terra Nova Bay in Antarctica during November and
1856 December 2000, J. Geophys. Res., 107(D23), 4722, doi:10.1029/2002JD002057, 2002.

1857 Sprovieri, F., N. Pirrone, K. Gärfeldt, and J. Sommar, Mercury measurements in the marine
1858 boundary layer along a 6000 km cruise path around the Mediterranean Sea, Atmos. Environ., 37
1859 suppl., S63-S71, 2003.

1860 Sprovieri, F., Pirrone, N., Ebinghaus, R., Kock, H., and Dommergue, A.: A review of worldwide
1861 atmospheric mercury measurements, Atmos. Chem. Phys., 10(17), 8245-8265, 2010b.
1862
1863 Stamenkovic, J., Lyman, S., and Gustin, M. S.: Seasonal and diel variation of atmospheric
1864 mercury concentrations in the Reno (Nevada, USA) airshed, Atmos. Environ., 41(31), 6662-
1865 6672, 2007.
1866
1867 Steffen, A., Douglas, T., Amyot, M., Ariya, P., Aspmo, K., Berg, T., Bottenheim, J., Brooks, S.,
1868 Cobbett, F., Dastoor, A. and Dommergue, A.: A synthesis of atmospheric mercury depletion
1869 event chemistry in the atmosphere and snow, Atmos. Chem. Phys., 8(6), 1445-1482, 2008.
1870
1871 Steffen, A., Bottenheim, J., Cole, A., Douglas, T.A., Ebinghaus, R., Friess, U., Netcheva, S.,
1872 Nghiem, S., Sihler, H. and Staebler, R.: Atmospheric mercury over sea ice during the OASIS-
1873 2009 campaign, Atmos. Chem. Phys., 13, 7007–7021, 2013.
1874
1875 Strode, S. A., L. Jaegle, N. E. Selin, D. J. Jacob, R. J. Park, R. M. Yantosca, R. P. Mason, and F.
1876 Slemr (2007), Air-sea exchange in the global mercury cycle, Global Biogeochem. Cycles, 21,
1877 GB1017, doi:10.1029/2006GB002766.
1878
1879 Subir, M., Ariya, P. A., and Dastoor, A. P.: A review of uncertainties in atmospheric modeling of
1880 mercury chemistry I. Uncertainties in existing kinetic parameters – fundamental limitations and
1881 the importance of heterogeneous chemistry, Atmos. Environ., 45, 5664–5676, 2011.

1882 Swartzendruber, P. C., D. Chand, D. A. Jaffe, J. Smith, D. Reidmiller, L. Gratz, J. Keeler, S.
1883 Strode, L. Jaegle, and R. Talbot (2008), Vertical distribution of mercury, CO, ozone, and aerosol
1884 scattering coefficient in the Pacific Northwest during the spring 2006 INTEX-B campaign, J.
1885 Geophys. Res., 113, D10305, doi:10.1029/2007JD009579.
1886
1887 Swartzendruber, P.C., Jaffe, D.A., Prestbo, E.M., Weiss-Penzias, P., Selin, N.E., Park, R., Jacob,
1888 D.J., Strode, S. and Jaegle, L.: Observations of reactive gaseous mercury in the free troposphere
1889 at the Mount Bachelor Observatory, J. Geophys. Res. Atmos., 111(D24301),
1890 doi:10.1029/2006JD007415, 2006.
1891
1892 Talbot, R., H. Mao, E. Scheuer, J. Dibb, and M. Avery (2007), Total Depletion of Hg° in the
1893 Upper Troposphere - Lower Stratosphere, *Geophys. Res. Lett.,* 34, L23804,
1894 doi:10.1029/2007GL031366.
1895

Talbot, R., H. Mao, E. Scheuer, J. Dibb, M. Avery, E. Browell, G. Sachse, S. Vay, D. Blake, G. Huey, and H. Fuelberg (2008), Factors influencing the large-scale distribution of Hg° in the Mexico City area and over the North Pacific, *Atmos. Chem. Phys. 8*, 2103-2114.

Temme, C., F. Slemr, R. Ebinghaus, J.W. Einax, Distribution of mercury over the Atlantic Ocean in 1996 and 1999–2001, Atmos. Environ., 37, 1889–1897, 2003a.

Temme, C., J.W. Einax , R. Ebinghaus, and W. H. Schroeder, Measurements of mercury species at a coastal site in the Antarctic and over the South Atlantic Ocean in the polar summer, Environ. Sci. Technol., 37, 1, 22 – 31, 2003b.

Timonen, H., J. L. Ambrose, and D. A. Jaffe, Oxidation of elemental Hg in anthropogenic and marine airmasses, Atmos. Chem., Phys., 13, 2827–2836, 2013.

Tseng, C.M., C.S. Liu, and C. Lamborg (2012) Seasonal changes in gaseous elemental mercury in relation to monsoon cycling over the northern South China Sea, *Atmospheric Chemistry and Physics*, 12, 7341-7350.

Turekian, V. C.; Van Dingenen, R. Inorganic bromine in the marine boundary layer: a critical review, *Atmos. Chem. Phys.*, *3*, 1301-1336, 2003.

UNEP, Global Mercury Assessment 2013: Sources, Emissions, Releases and Environmental Transport. UNEP Chemicals Branch, Geneva, Switzerland, 2013.

Valente, R. J., Shea, C., Humes, K. L., and Tanner, R. L.: Atmospheric mercury in the Great Smoky Mountains compared to regional and global levels, Atmos. Environ., 41(9), 1861-1873, 2007.

Wan, Q., Feng, X., Lu, J., Zheng, W., Song, X., Han, S., and Xu, H.: Atmospheric mercury in Changbai Mountain area, northeastern China I. The seasonal distribution pattern of total gaseous mercury and its potential sources, Environ. Res., 109(3), 201-206, 2009a.

Wan, Q., Feng, X., Lu, J., Zheng, W., Song, X., Li, P., Han, S. and Xu, H., Atmospheric mercury in Changbai Mountain area, northeastern China II. The distribution of reactive gaseous mercury and particulate mercury and mercury deposition fluxes, Environ. Res., 109(6), 721-727, 2009b.

Wang, F., A. Saiz-Lopez, A. S. Mahajan,, J. C. Gómez Martín,, D. Armstrong, M. Lemes, T. Hay, and C. Prados-Roman, Enhanced production of oxidised mercury over the tropical Pacific Ocean: a key missing oxidation pathway, Atmos. Chem. Phys., 14, 1323–1335, 2014.。

Wang, Y., Huang, J., Hopke, P. K., Rattigan, O. V., Chalupa, D. C., Utell, M. J., and Holsen, T. M.: Effect of the shutdown of a large coal-fired power plant on ambient mercury species, Chemosphere, 92(4), 360-367, 2013.

Weigelt, A., Ebinghaus, R., Manning, A. J., Derwent, R. G., Simmonds, P. G., Spain, T. G., Jennings, S. G., and Slemr, F.: Analysis and interpretation of 18 years of mercury observations

since 1996 at Mace Head at the Atlantic Ocean coast of Ireland, Atmos. Environ. 100, 85–93, 2015.

Weiss-Penzias, P. S., E. J. Williams, B. M. Lerner, T. S. Bates, C. Gaston, K. Prather, A. Vlasenko, and S. M. Li (2013), Shipboard measurements of gaseous elemental mercury along the coast of Central and Southern California. J. Geophys. Res. Atmos., 118, 208–219, doi:10.1029/2012JD018463.

Weiss-Penzias, P., Amos, H.M., Selin, N.E., Gustin, M.S., Jaffe, D.A., Obrist, D., Sheu, G.R. and Giang, A.: Use of a global model to understand speciated atmospheric mercury observations at five high-elevation sites, Atmos. Chem. Phys., 15(3), 1161-1173, 2015.

Weiss-Penzias, P., D. A. Jaffe, A. McClintick, E. M. Presbo, and M. S. Landis, Gaseous elemental mercury in the Marine Boundary Layer: Evidence for rapid removal in anthropogenic pollution, Environ. Sci. Technol., 3755 – 3763, 37, 2003.

Weiss-Penzias, P., Gustin, M. S., and Lyman, S. N.: Observations of speciated atmospheric mercury at three sites in Nevada: Evidence for a free tropospheric source of reactive gaseous mercury, J. Geophys. Res. Atmos., 114(D14), 2009.

Weiss-Penzias, P., Jaffe, D., Swartzendruber, P., Hafner, W., Chand, D., and Prestbo, E.: Quantifying Asian and biomass burning sources of mercury using the Hg/CO ratio in pollution plumes observed at the Mount Bachelor Observatory, Atmos. Environ., 41(21), 4366-4379, 2007.

Weiss-Penzias, P.S., Gay, D.A., Brigham, M.E., Parsons, M.T., Gustin, M.S. and ter Schure, A.: Trends in mercury wet deposition and mercury air concentrations across the US and Canada. Sci. Total Environ., in press, 2016.

Williston, S. H. *(1968), Mercury in the atmosphere, J. Geophys. Res., 73(22), 7051–7055, doi:*10.1029/JB073i022p07051.

Witt, M. L. I., Mather, T. A., Baker, A. R., De Hoog, J. C. M., and Pyle, D. M.: Atmospheric trace metals over the south-west Indian Ocean: total gaseous mercury, aerosol trace metal concentrations and lead isotope ratios, Mar. Chem., 121, 2–16, 2010.

Witt, M. L. I., Meheran, N., Mather, T. A., De Hoog, J. C. M., and Pyle, D. M.: Aerosol trace metals, particle morphology and total gaseous mercury in the atmosphere of Oxford, UK, Atmos. Environ., 44(12), 1524-1538, 2010.

Won, J. H., Park, J. Y., and Lee, T. G., Mercury emissions from automobiles using gasoline, diesel, and LPG, Atmos. Environ., 41, 7547-7552, 2007.

Xia, C., Z. Xie, and L. Sun, Atmospheric mercury in the marine boundary layer along a cruise path from Shanghai, China to Prydz Bay, Antarctica, Atmos. Environ., 44, 1815-1821, 2010.

1988 Xiu, G., Cai, J., Zhang, W., Zhang, D., Büeler, A., Lee, S., Shen, Y., Xu, L., Huang, X. and
1989 Zhang, P.: Speciated mercury in size-fractionated particles in Shanghai ambient air, Atmos.
1990 Environ., 43(19), 3145-3154, 2009.
1991
1992 Xu, L., Chen, J., Yang, L., Niu, Z., Tong, L., Yin, L., and Chen, Y.: Characteristics and sources
1993 of atmospheric mercury speciation in a coastal city, Xiamen, China, Chemosphere, 119, 530-539,
1994 2015.
1995
1996 Xu, X. and Akhtar, U. S.: Identification of potential regional sources of atmospheric total
1997 gaseous mercury in Windsor, Ontario, Canada using hybrid receptor modeling, Atmos. Chem.
1998 Phys., 10(15), 7073-7083, 2010.
1999
2000 Xu, X., Akhtar, U., Clark, K., and Wang, X.: Temporal variability of atmospheric total gaseous
2001 mercury in Windsor, ON, Canada, Atmosphere, 5(3), 536-556, 2014.
2002 Yang, Y., Chen, H., and Wang, D.: Spatial and temporal distribution of gaseous elemental
2003 mercury in Chongqing, China, Environ. Monit. Assess., 156(1-4), 479-489, 2009.
2004
2005 Yatavelli, R. L., Fahrni, J. K., Kim, M., Crist, K. C., Vickers, C. D., Winter, S. E., and Connell,
2006 D. P.: Mercury, PM 2.5 and gaseous co-pollutants in the Ohio River Valley region: Preliminary
2007 results from the Athens supersite, Atmos. Environ., 40(34), 6650-6665, 2006.
2008
2009 Yu, J. et al., High variability of atmospheric mercury in the summertime boundary layer through
2010 the central Arctic Ocean. Scientific Reports, 4, 6091, DOI:10.1038/srep06091, 2014.
2011
2012 Zhang, H., Fu, X. W., Lin, C.-J., Wang, X., and Feng, X. B.: Observation and analysis of
2013 speciated atmospheric mercury in Shangri-La, Tibetan Plateau, China, Atmos. Chem. Phys., 15,
2014 653-665, doi:10.5194/acp-15-653-2015, 2015.
2015
2016 Zhang, L., Wright L.P., and Blanchard P., 2009. A review of current knowledge concerning dry
2017 deposition of atmospheric mercury. Atmospheric Environment, 43, 5853-5864.
2018
2019 Zhang, L., Blanchard P., Johnson D., Dastoor A., Ryzhkov A., Lin C.-J., Vijayaraghavan K.,
2020 Gay D., Holsen T.M., Huang J., Graydon J.A., St. Louis V.L., Castro M.S., Miller E.K., Marsik
2021 F., Lu J., Poissant L., Pilote M., and Zhang K.M., 2012. Assessment of modelled mercury
2022 deposition over the Great Lakes region. Environmental Pollution, 161, 272-283.
2023
2024 Zhang, L., Wang, S. X., Wang, L., and Hao, J. M.: Atmospheric mercury concentration and
2025 chemical speciation at a rural site in Beijing, China: implications of mercury emission sources,
2026 Atmos. Chem. Phys., 13(20), 10505-10516, 2013.
2027
2028 Zhang, Y., Jacob, D.J., Horowitz, H.M., Chen, L., Amos, H.M., Krabbenhoft, D.P., Slemr, F., St.
2029 Louis, V.L. and Sunderland, E.M.: Observed decrease in atmospheric mercury explained by
2030 global decline in anthropogenic emissions, Proceed. Natl, Acad. Sci., 113(3), 526-531, 2016.
2031

2032　Zhu, J., Wang, T., Talbot, R., Mao, H., Hall, C.B., Yang, X., Fu, C., Zhuang, B., Li, S., Han, Y.
2033　and Huang, X.: Characteristics of atmospheric total gaseous mercury (TGM) observed in urban
2034　Nanjing, China, Atmos. Chem. Phys., 12(24), 12103-12118, 2012.
2035

2036　Zielonka, U., Hlawiczka, S., Fudala, J., Wängberg, I., and Munthe, J.: Seasonal mercury
2037　concentrations measured in rural air in Southern Poland: Contribution from local and regional
2038　coal combustion, Atmos. Environ., 39(39), 7580-7586, 2005.
2039

2040 Table 1: Summary of predominant temporal patterns of speciated atmospheric mercury at
2041 continental sites in the northern hemisphere

|	Diurnal variation	Seasonal variation
TGM/GEM		
Rural	Daytime maximum, nighttime minimum	Winter-spring maximum and summer-fall minimum
Urban	Nighttime maximum, daytime minimum	No predominant pattern
High elevation	Daytime maximum, nighttime minimum	Winter-spring maximum and summer-fall minimum
GOM		
Rural	Midday to late afternoon maximum,	No predominant pattern
Urban	nighttime minimum	Spring or summer maximum
High elevation	*Exception: nighttime maximum at urban and elevated sites	No predominant pattern
PBM		
Rural	No predominant pattern	Maximum during heating season
Urban	No predominant pattern	Maximum during heating season *Exception: summer maximum
High elevation	No predominant pattern	Maximum during heating season

2042
2043
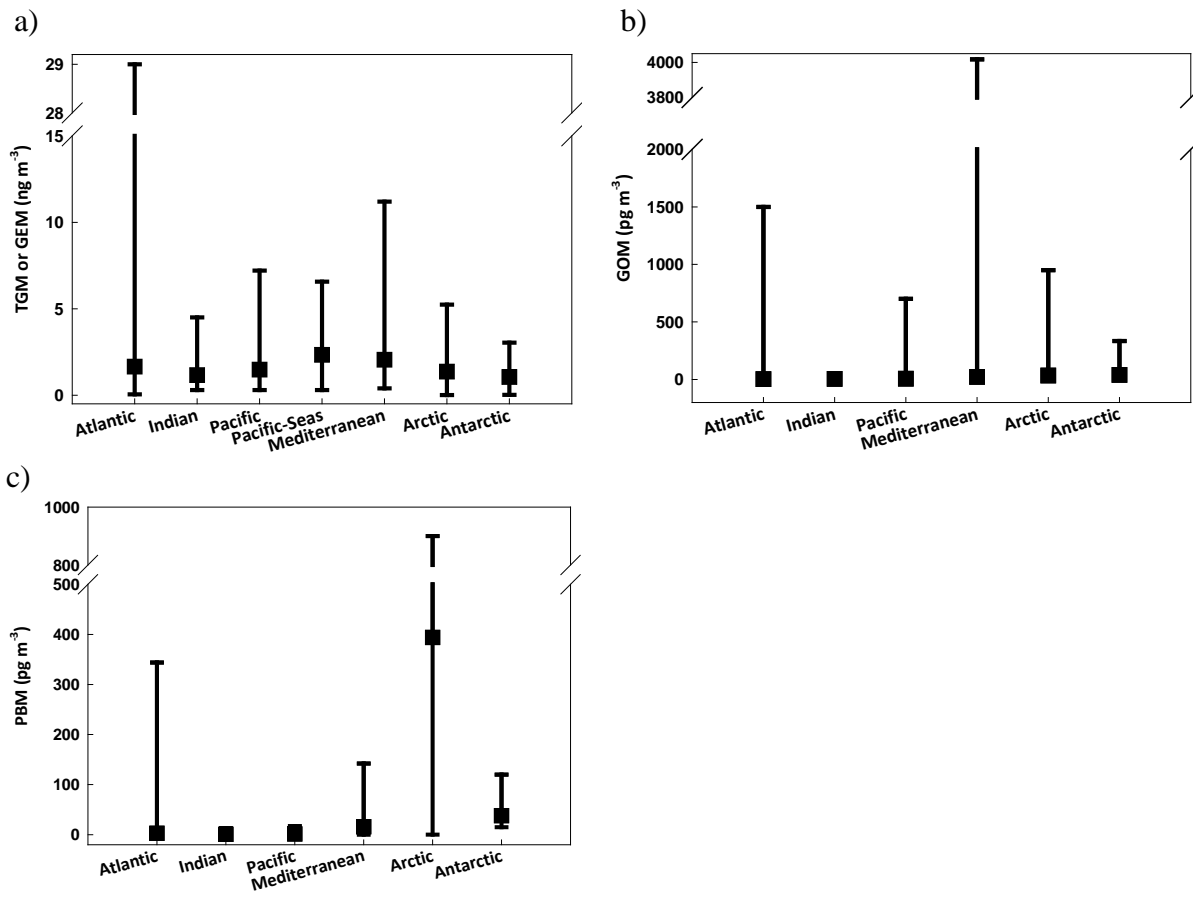
a)

b)

c)

2044
2045
2046   Figure 1. Means and ranges of TGM/GEM (a), GOM (b), and PBM (c) concentrations,
2047   estimated from the values in the literature as shown in Tables S1 – S3, over the Atlantic,
2048   Indian, Pacific, seas over the West Pacific (denoted as Pacific-Seas, only TGM/GEM in this
2049   category), seas in the Mediterranean region (denoted as Mediterranean), Arctic, and
Antarctica Ocean. The solid black squares represent the mean value and the lowest whisker
the minimum and the largest the maximum concentration in the region.

2050
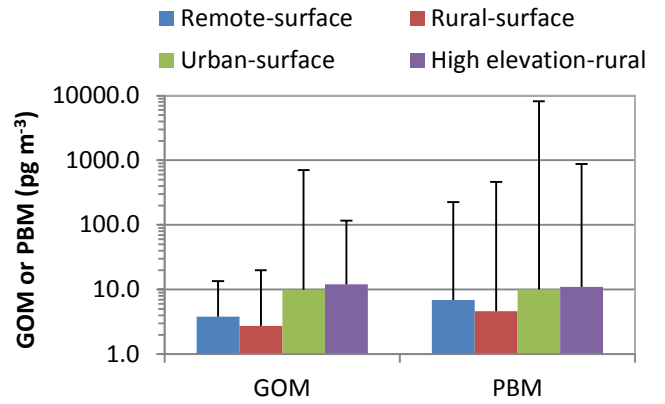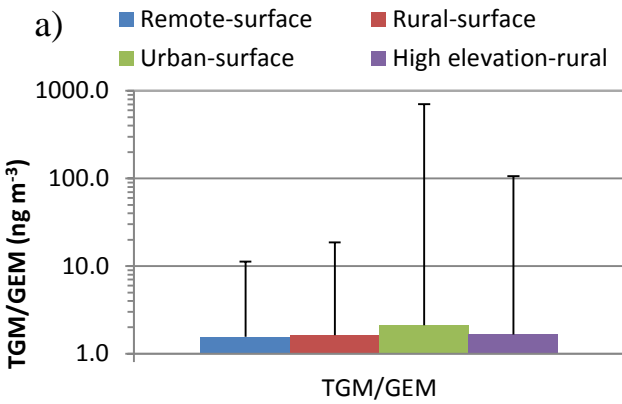
2051
2052
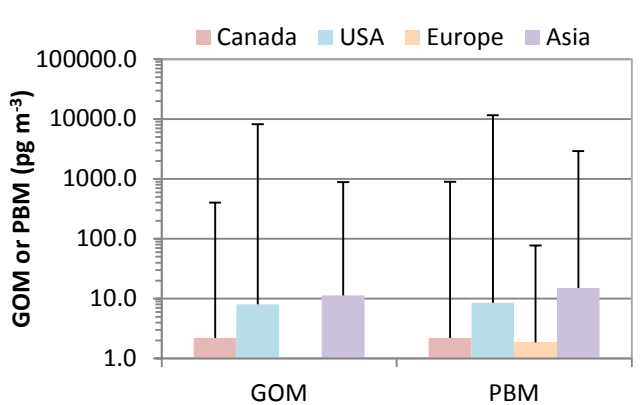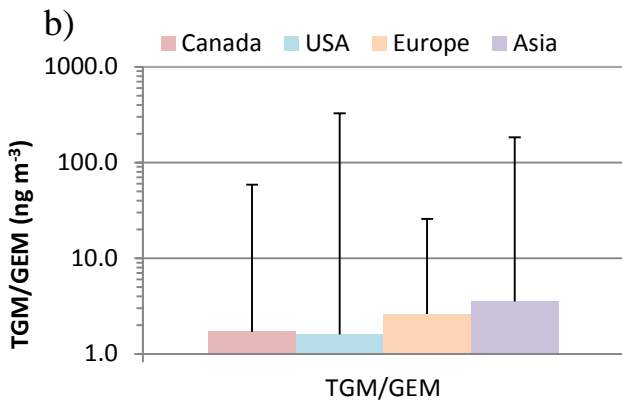
2053
2054
2055
2056 Figure 2. Median and range in TGM/GEM, GOM and PBM by site category (a) and by
2057 geographical region (b). Bar graph represents the median and error bar represents the maximum,
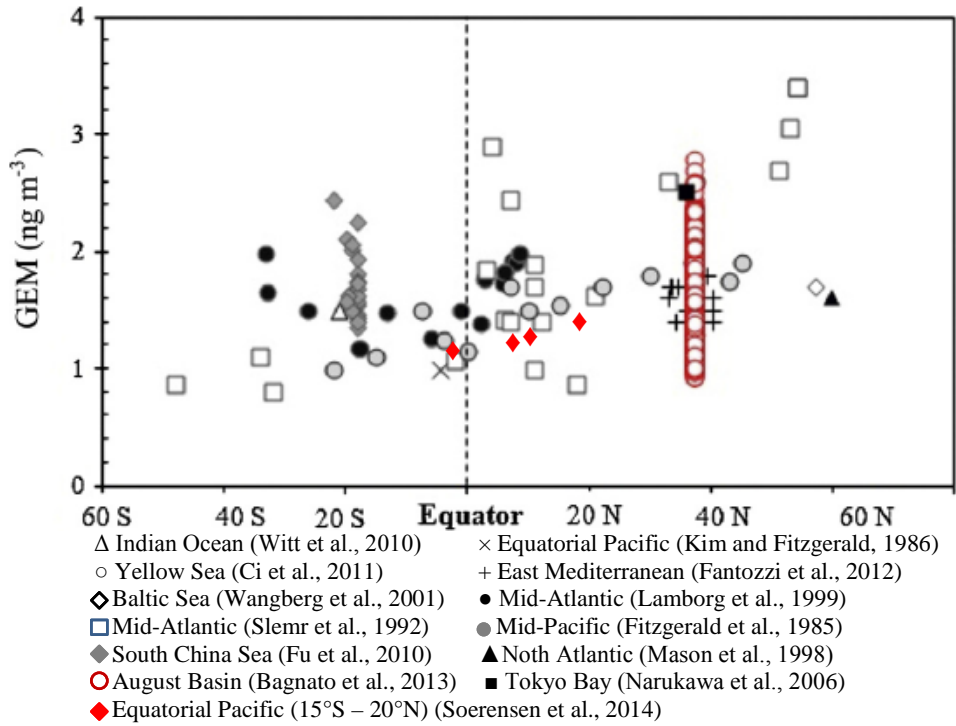2058 estimated from the values in the literature as shown in Tables S4 – S6.
2059
2060
2061
2062

Figure 3. Compiled values for several marine/oceanic environmental systems adapted mostly from Bagnato et al. (2013)

2093
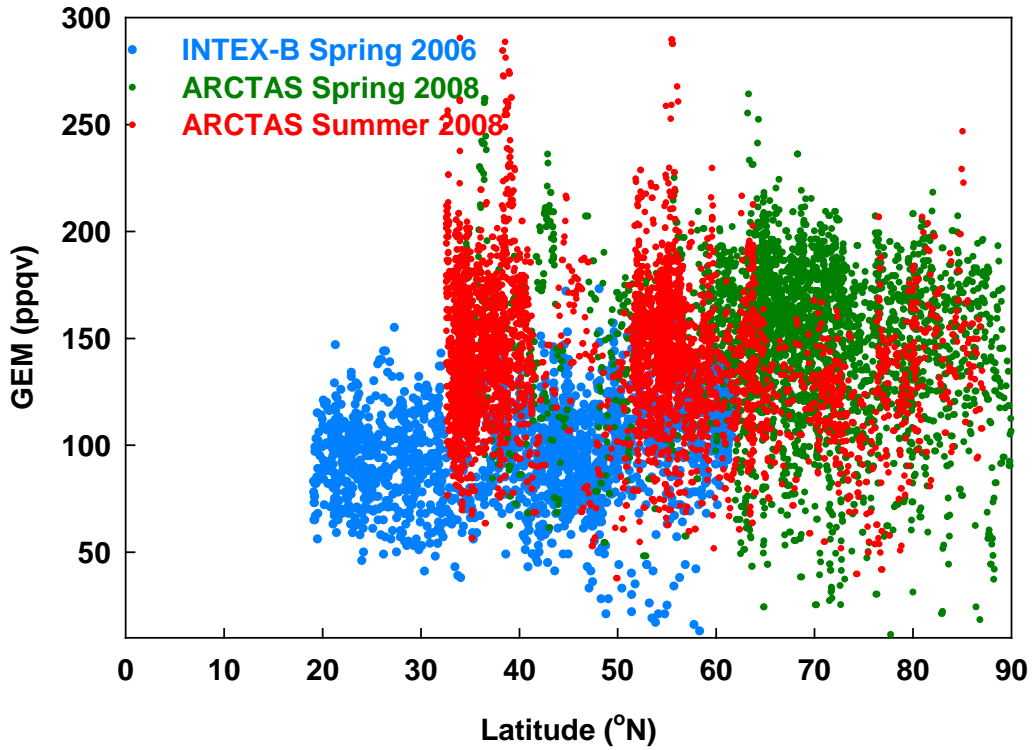2094
209˜
209
209
209
209
209
210

Figure 4. GEM (ppqv) from the INTEX-B in spring 2006 and ARCTAS in spring and summer 2008 (Data sources: Talbot et al., 2007, 2008; Mao et al., 2010).